Measurements and implications of high energy diffuse γ-ray emission from the Galactic plane

Xiaoyuan Huang

Purple Mountain Observatory, Chinese Academy of Science
On behalf of LHAASO collaborations

25/09@RICAP-24

Galactic cosmic rays

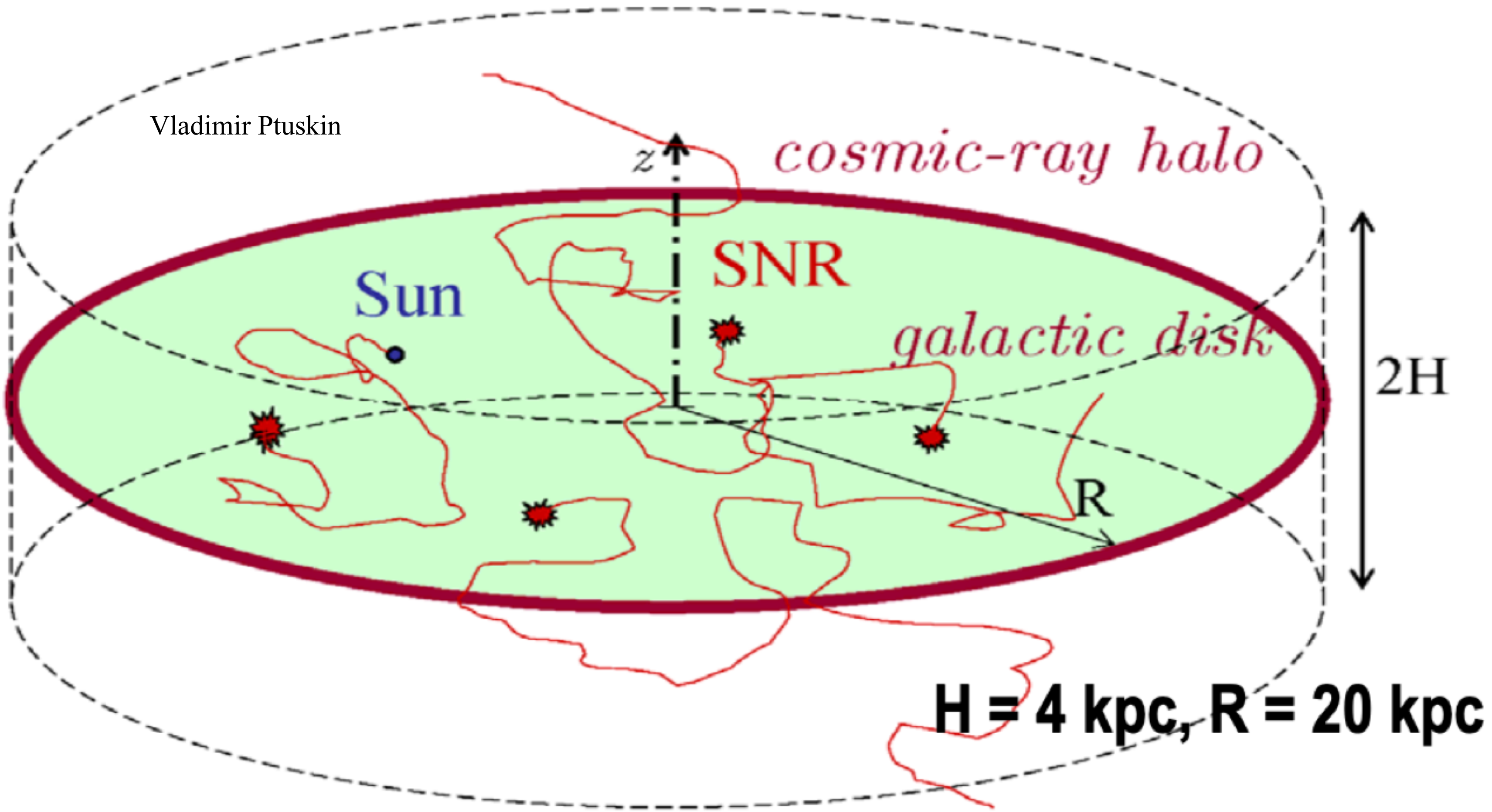

After acceleration, cosmic rays propagate in the galactic magnetic field, losing the information about their origin and forming a smooth background of cosmic rays.

Origins of Galactic diffuse γ rays

Fermi-LAT

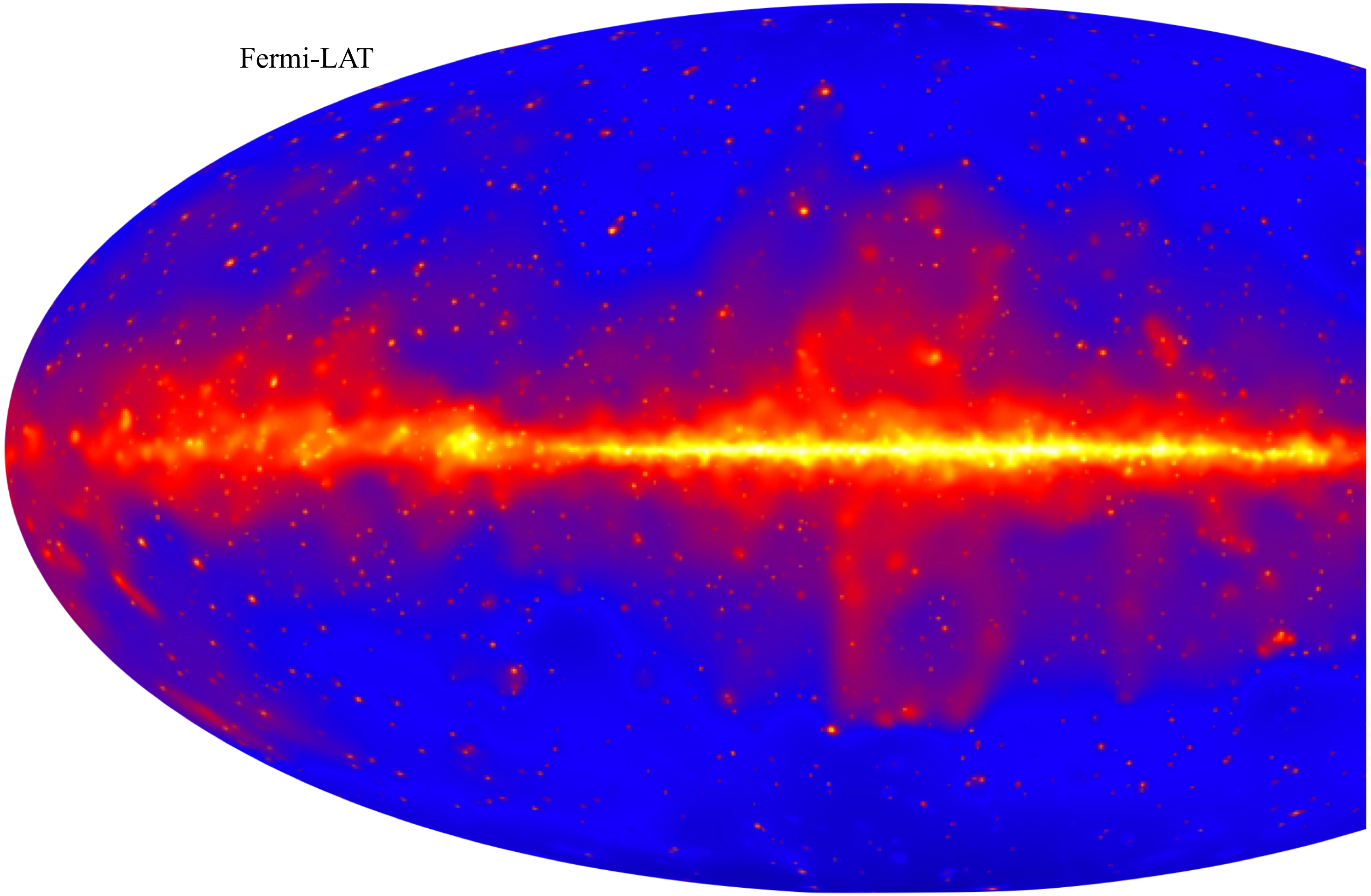

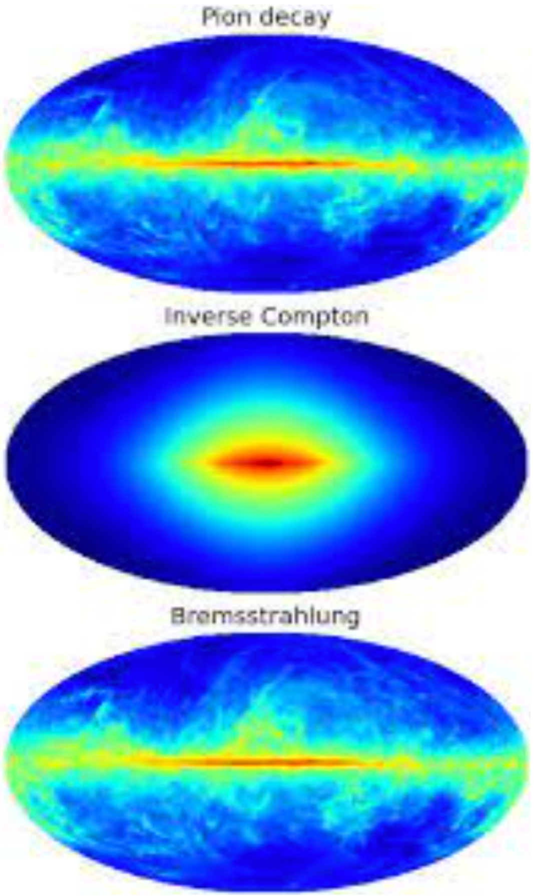

Cosmic rays interact with interstellar medium and radiation fields
to generate diffuse gamma-ray

Diffuse γ-ray emissions from space-based observations

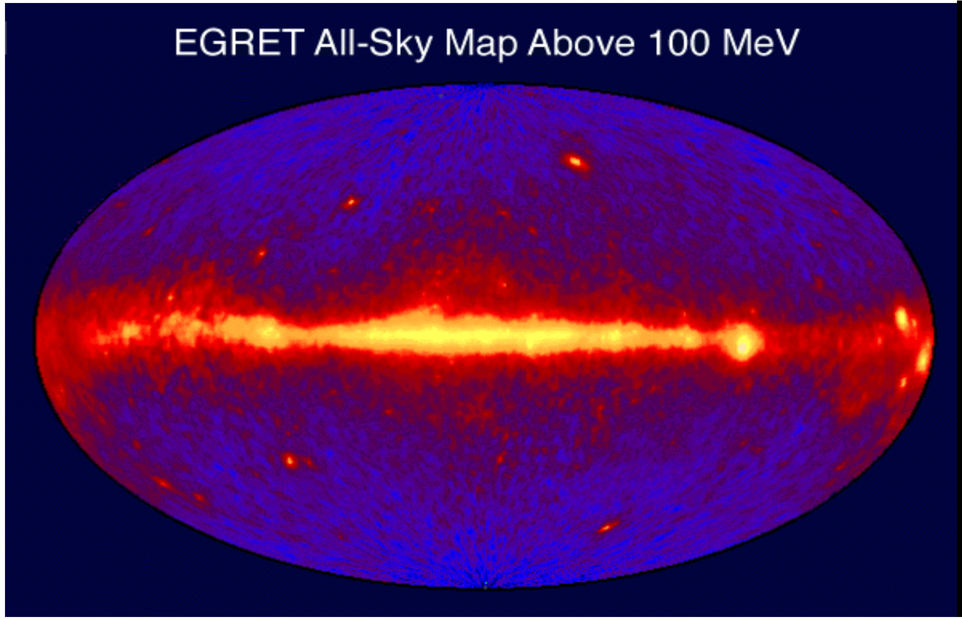

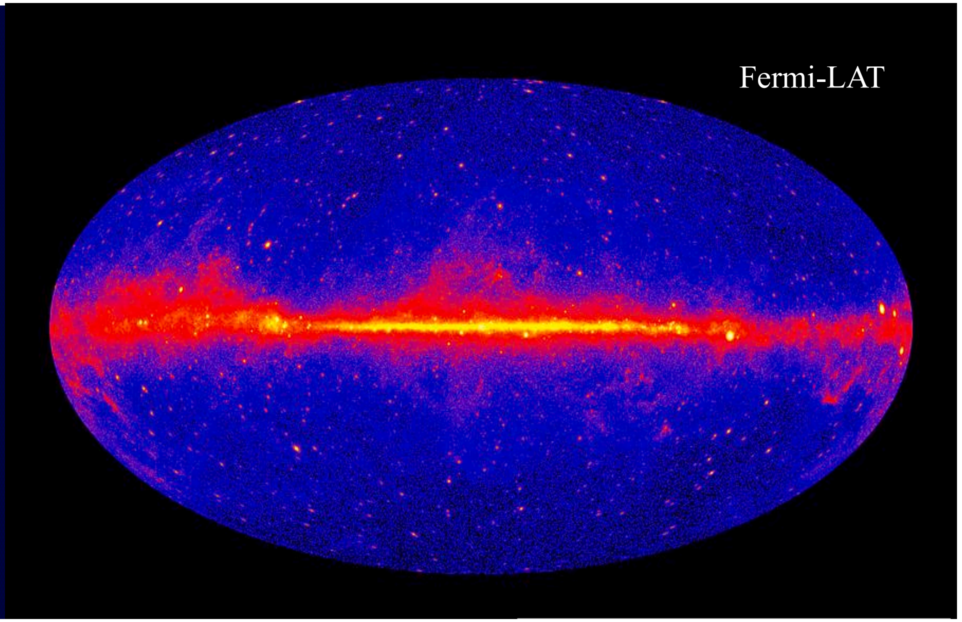

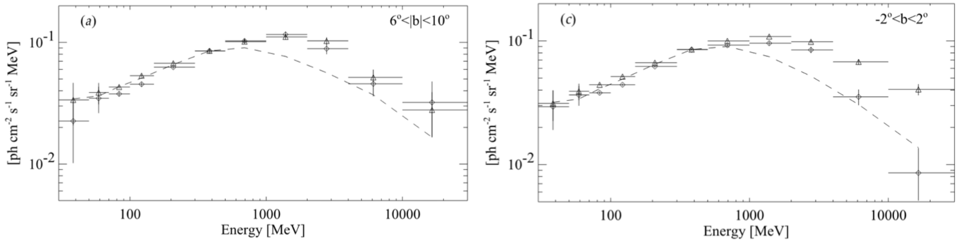

Hunter et al. 1997

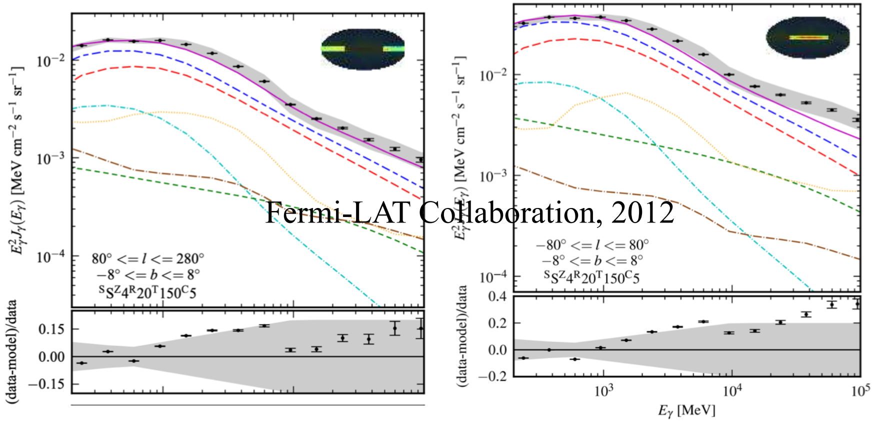

Fermi-LAT Collaboration, 2012

EGRET mapped an entire sky of gamma rays, and there are excesses above 1 GeV in different parts of regions.

Fermi-LAT's observations show a roughly consistent with anticipations, but in the inner galaxy, there are excesses above 1 GeV.

Diffuse γ-ray observations from ground-based facilities

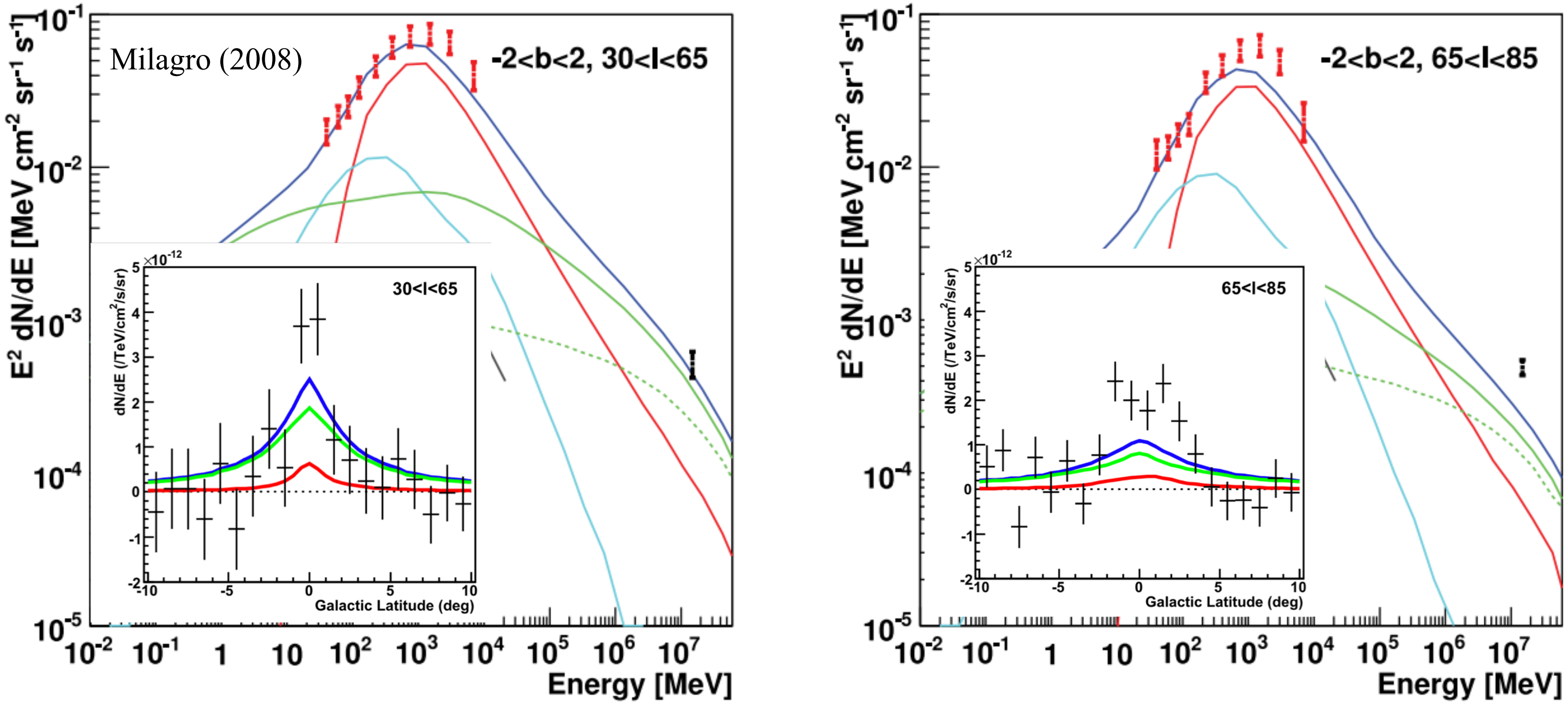

Milagro measured diffuse emissions in the Galactic plane around ~10 TeV, found excesses in the Cygnus region. However, source subtraction of Milagro is very limited.

Diffuse γ-ray observations from ground-based facilities

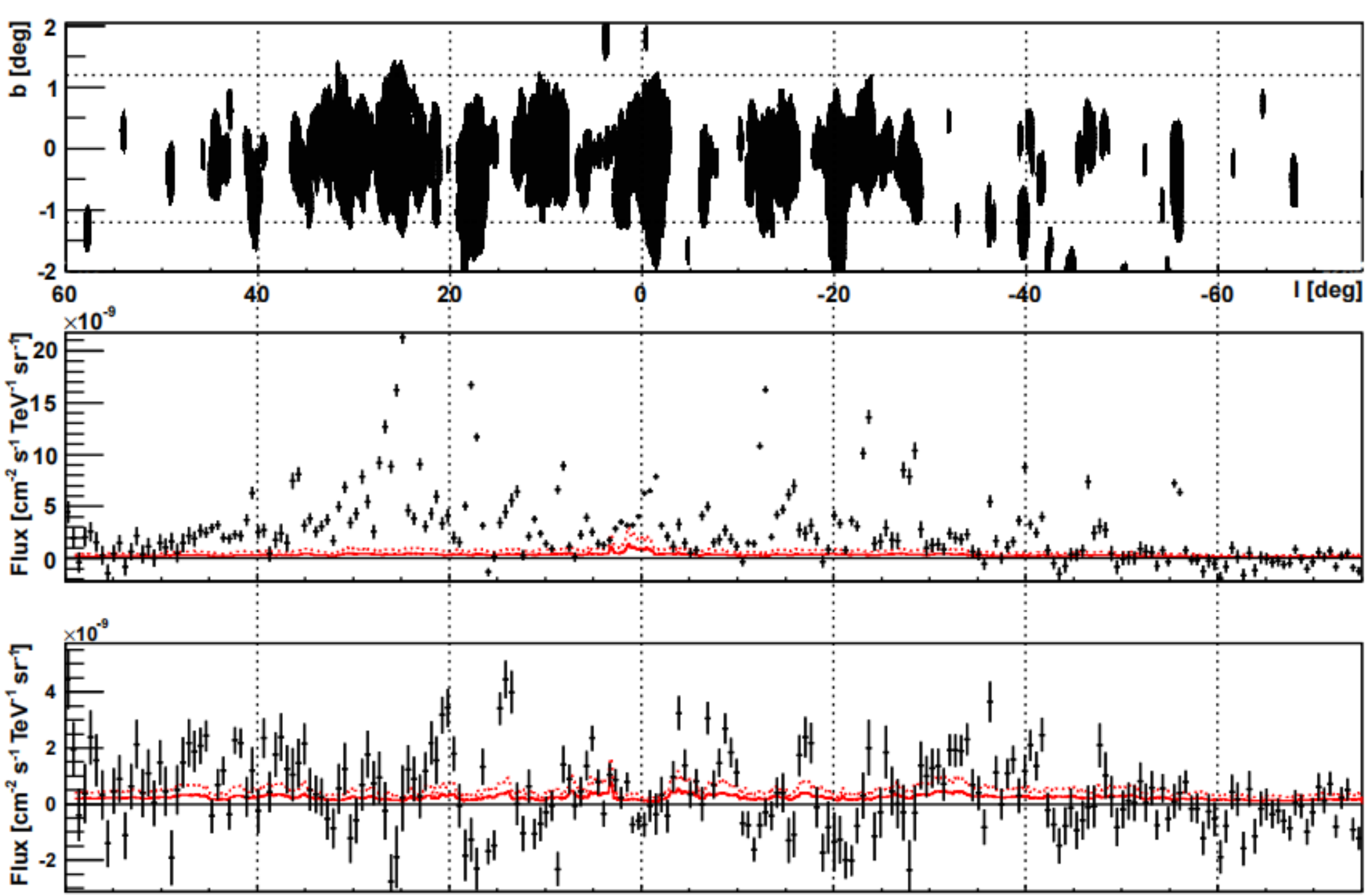

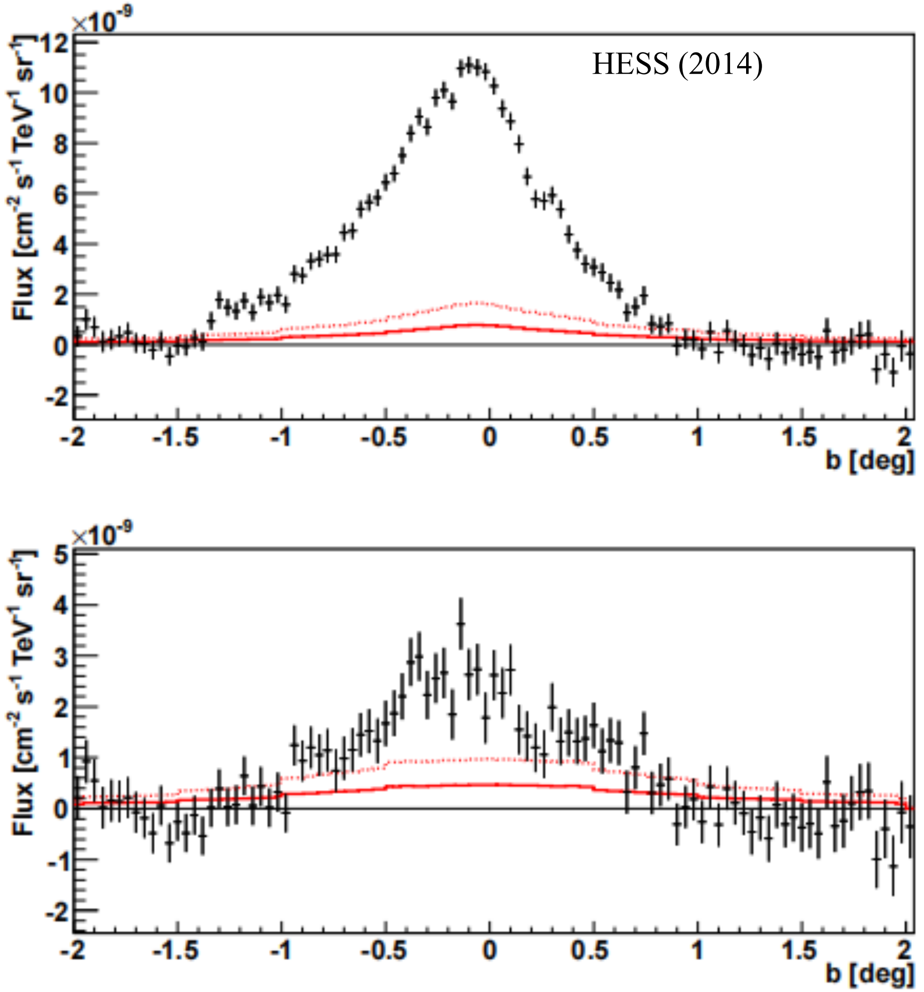

For the first time large-scale γ-ray emission along the Galactic Plane using imaging atmospheric Cherenkov telescopes has been observed. γ-ray emission from cosmic-ray interactions with the interstellar medium makes up a sizable fraction of the signal, but there is excess flux.

Diffuse γ-ray observations from ground-based facilities

ARGO-YBJ (2015)

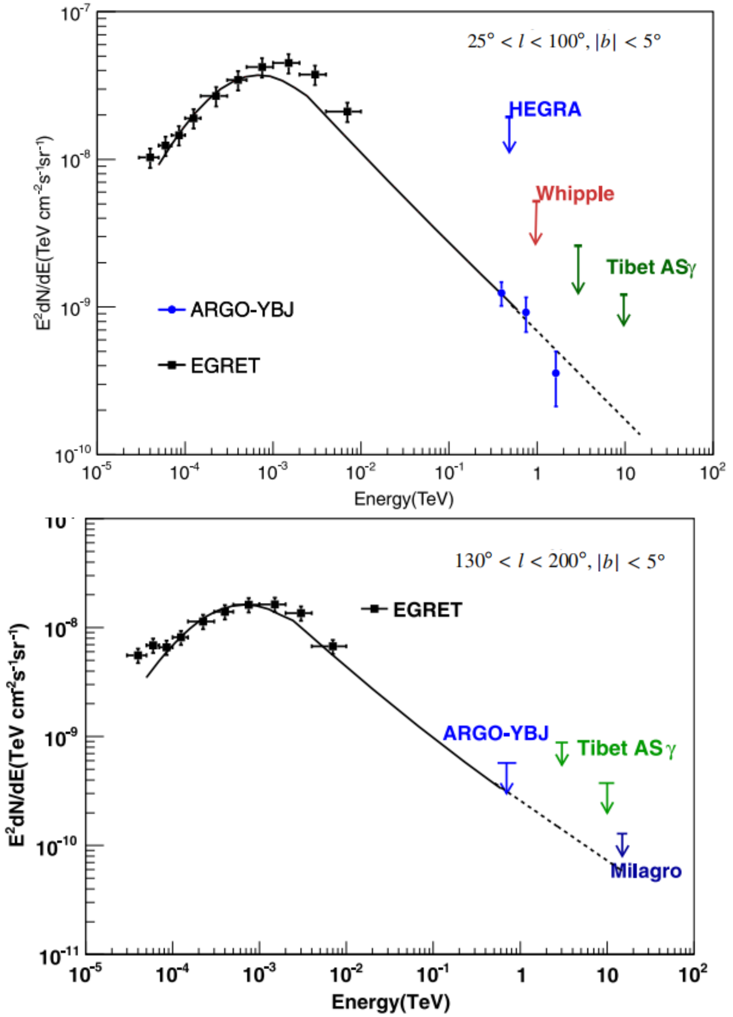

Tibet-ASγ (2021)

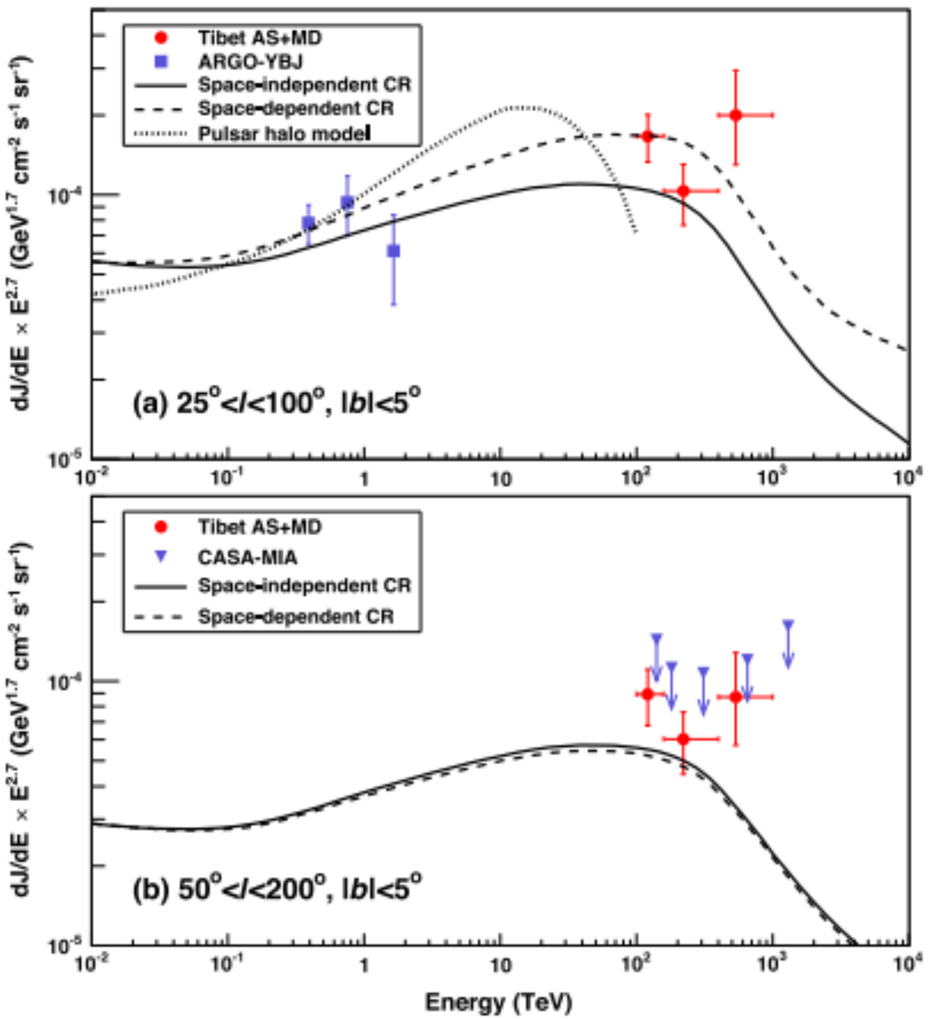

ARGO-YBJ measured diffuse emission from the inner Galaxy region, which is consistent with the extrapolation of Fermi-tuned model prediction

Tibet-ASγ measured diffuse emission above 100 TeV, and found excesses compared with the model prediction. Masking radius is 0.5 degree.

Wide-band diffuse emission measurements

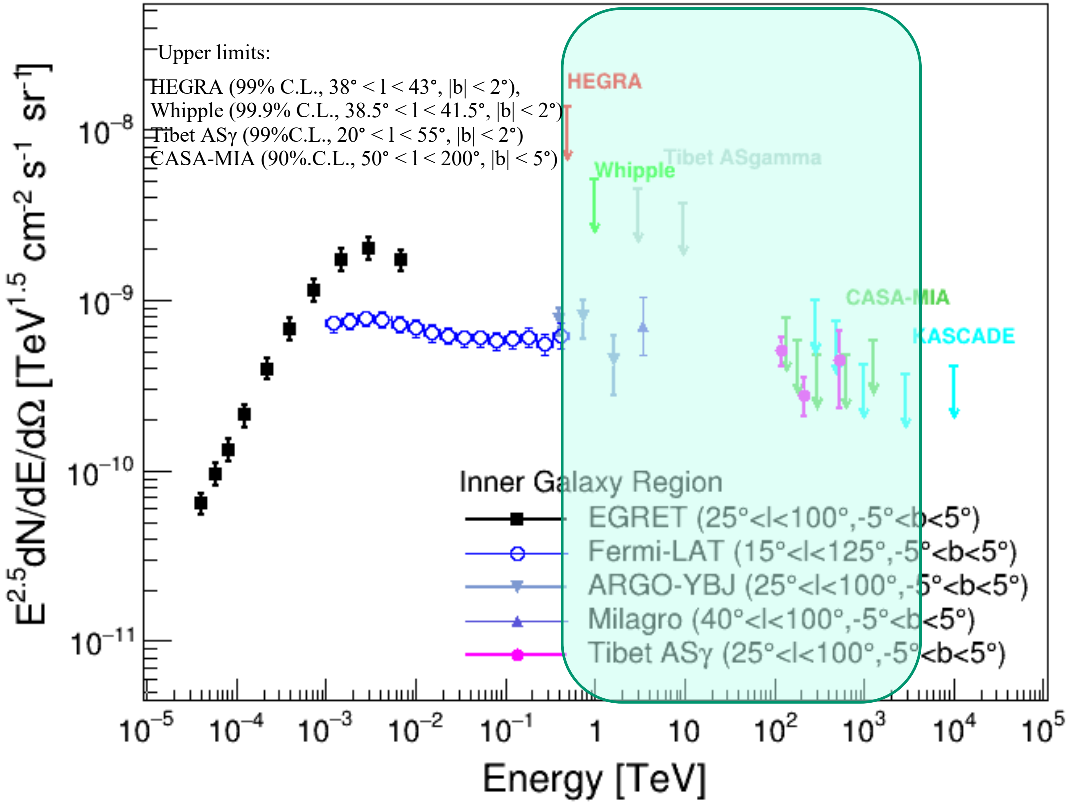

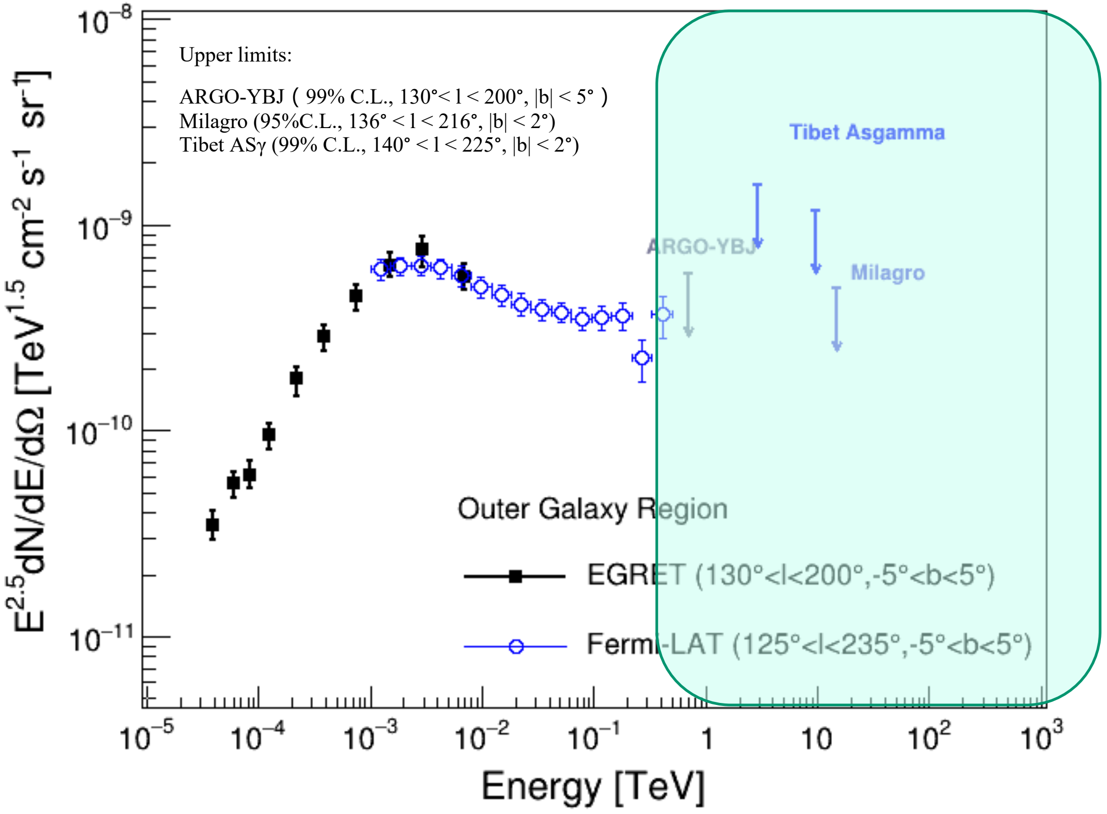

Comparison between prediction based on cosmic-ray properties and wide-band diffuse emission measurements are important for cosmic-ray investigation. However, usually diffuse emission measured by ground-based facilities are for different target regions, and in the outer galaxy region there is no detection yet.

LHAASO detector layout

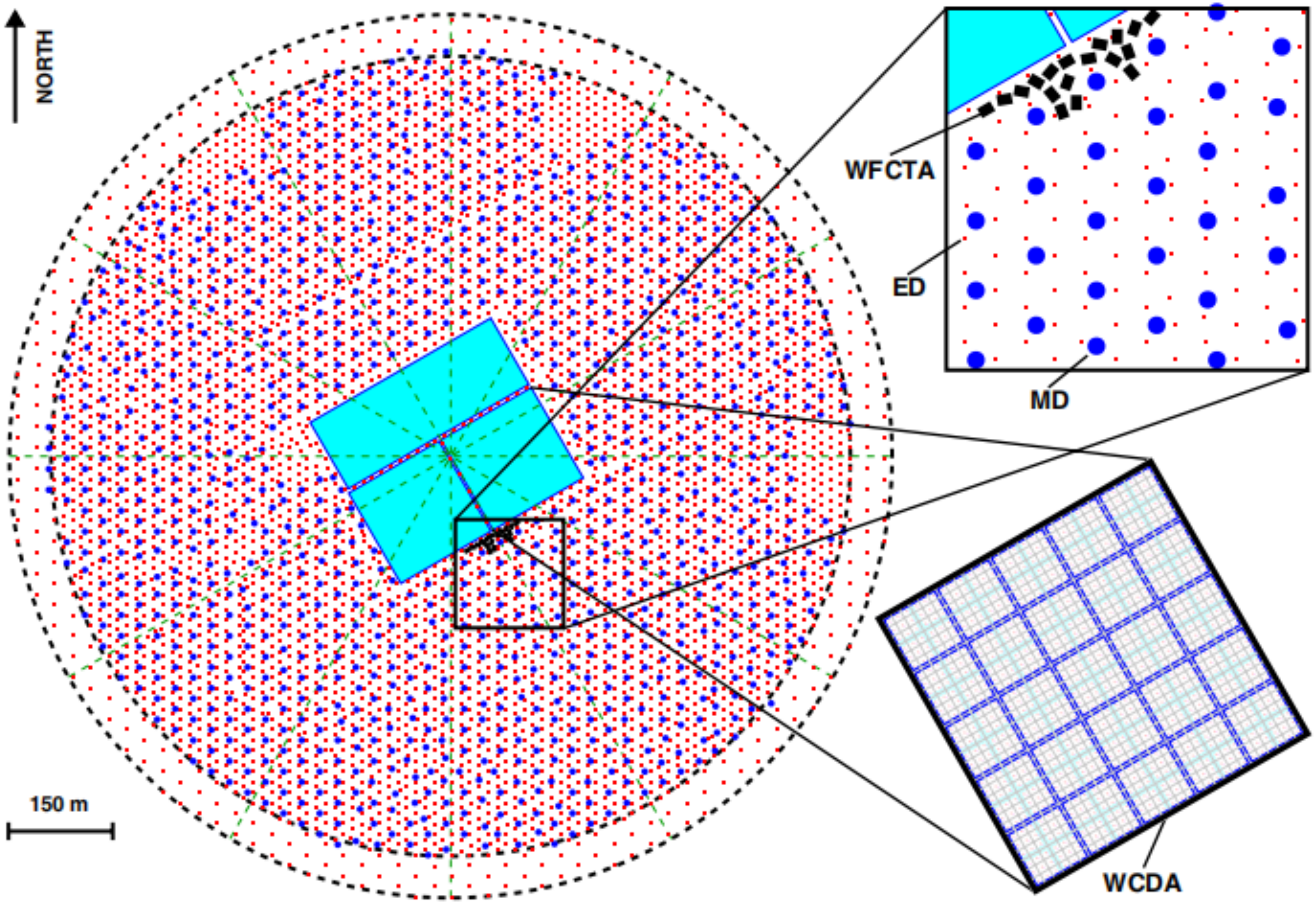

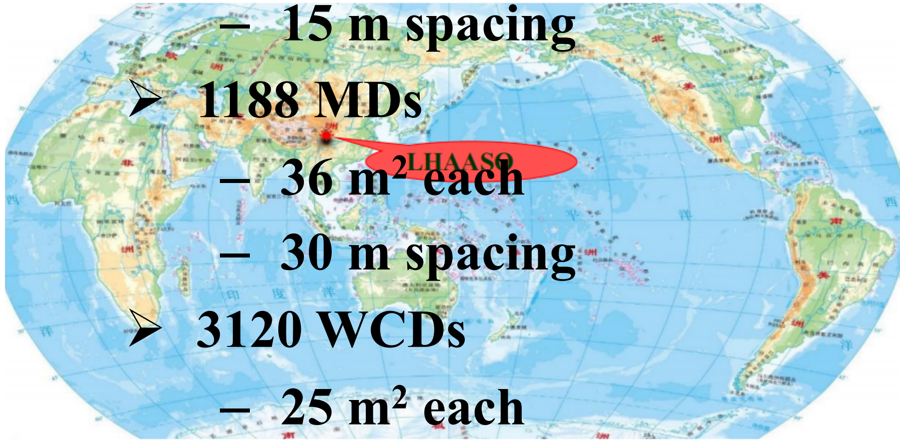

- 5195 EDs
  - 1 m² each
  - 15 m spacing
- 1188 MDs
  - 36 m² each
  - 30 m spacing
- 3120 WCDs
  - 25 m² each
- 18 WFCTs

The large area and hybrid detection technique makes LHAASO a powerful facility for cosmic ray and gamma-ray observations in a wide energy range.

LHAASO-KM2A sky coverage

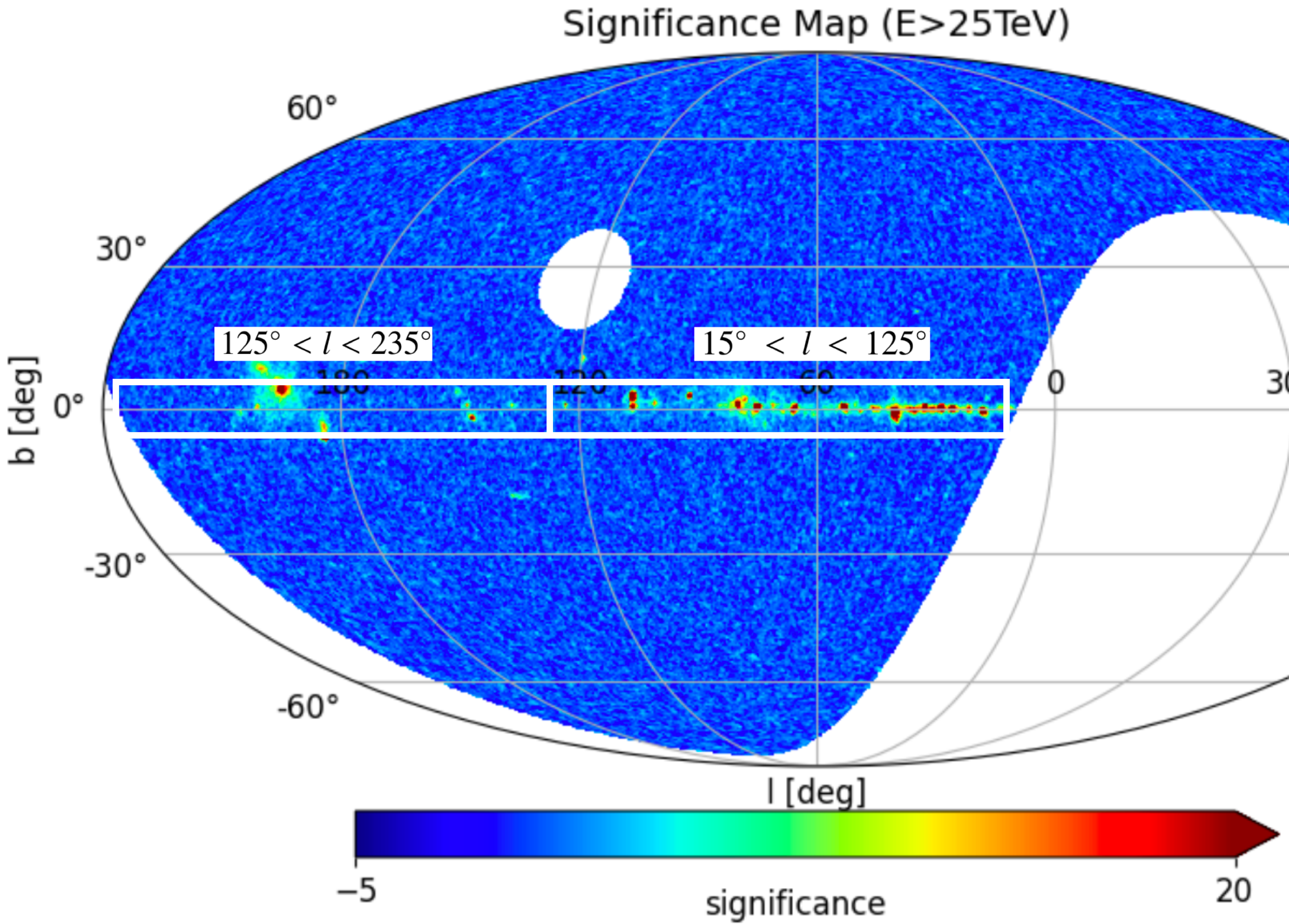

Gamma/CR discrimination

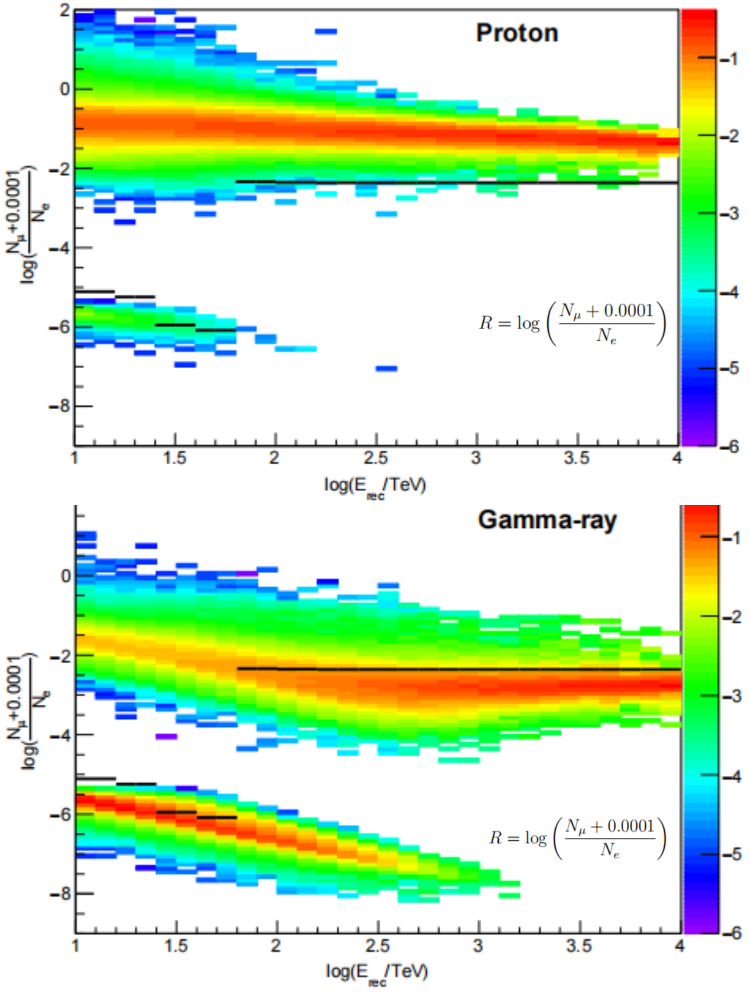

$\log_{10}(E_{rec}/\mathrm{TeV})$	R_{cut} for crab	R_{cut} for diffuse
1.0 – 1.2	−5.11	−5.00
1.2 – 1.4	−5.24	−3.20
1.4 – 1.6	−5.95	−5.96
1.6 – 1.8	−6.08	−6.17
1.8 – 2.0	−2.34	−2.50
2.0 – 2.2	−2.35	−2.69
2.2 – 2.4	−2.36	−2.79
2.4 – 2.6	−2.36	−2.74
2.6 – 2.8	−2.36	−2.75
2.8 – 3.0	−2.36	−2.79

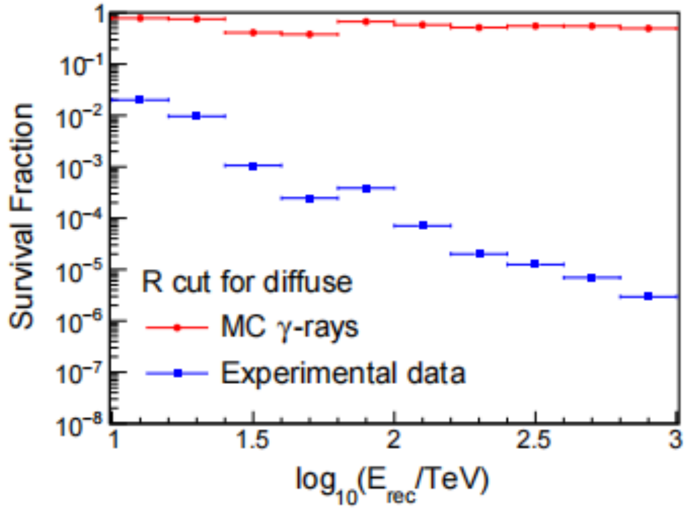

- Optimize R cuts from the standard point source analysis to enable a higher $Q=S/B^{1/2}$ factor for diffuse emission analysis
- Efficiencies change from ~90% to ~60% for gamma-ray events with energy above 100 TeV, but the contamination from cosmic-ray is strongly suppressed at very high energy

Background estimation

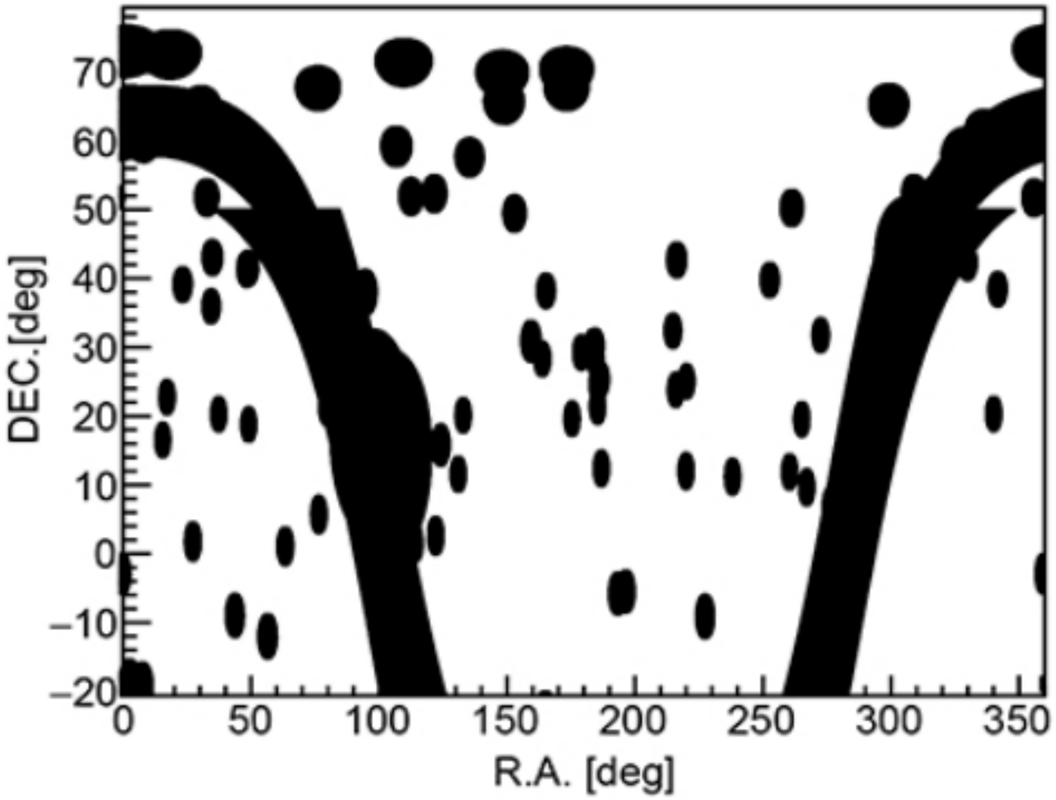

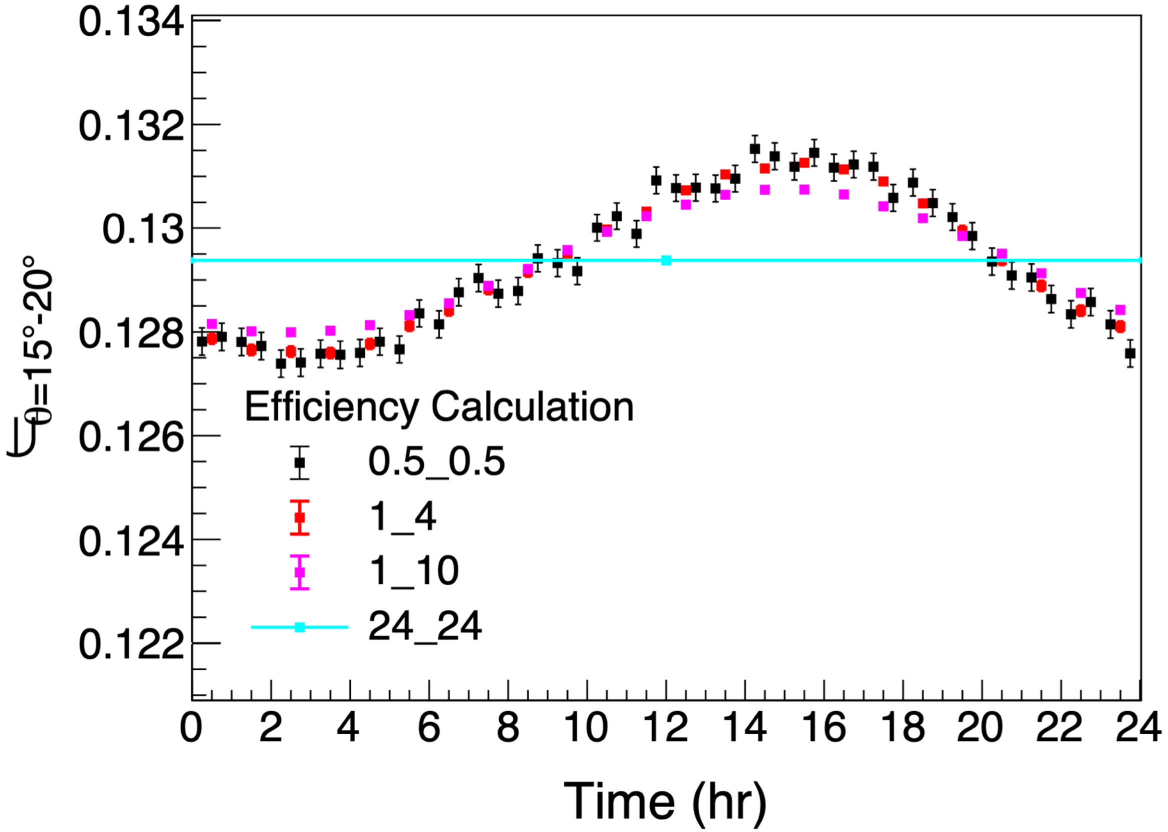

- Direct integral method: assuming the collecting efficiency's spatial distribution in the detector coordinates remains stable over a short period.
- Efficiencies do vary slightly with time, and thus a sliding window method is adopted (1_10 is used as benchmark, 1 hr step and +/-5 hr window)

Mask resolved sources

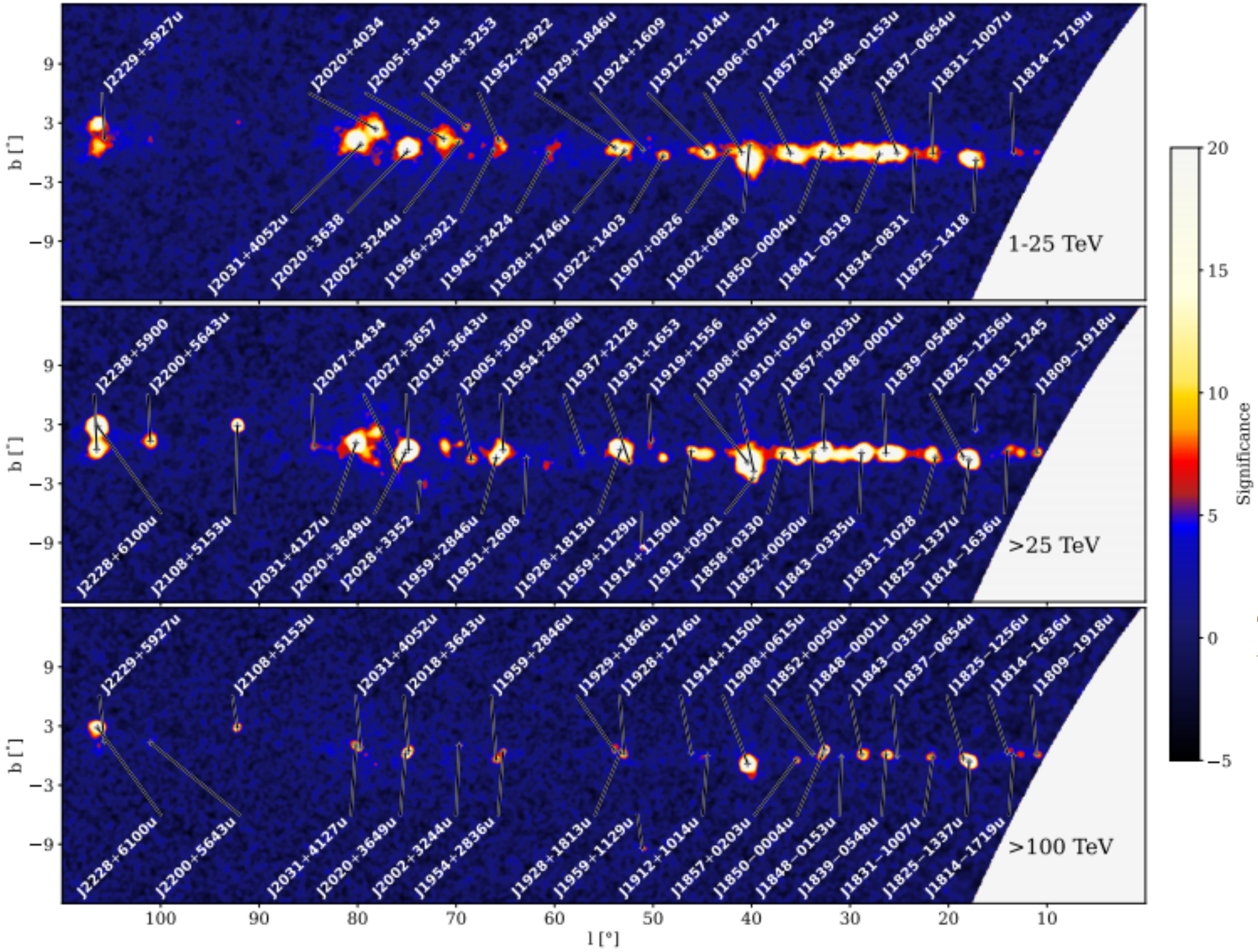

LHAASO first catalog (2024, ApJS)

LHAASO Collaboration. (PRL, 2023)

$$R_{\text{mask}} = n \cdot \sqrt{\sigma_{\text{psf}}^2 + \sigma_{\text{ext}}^2},$$

- Source catalogs: KM2A catalog + TeVCat
- For overlapping sources, KM2A parameters are used
- PSF of the lowest energy bin is used
- n=2.5 is chosen

Table 5: Proportion (%) of contamination (f_{cont}) of residual sources (LHAASOCat+TeVCat) to the DGE.

$\log_{10}\left(\frac{E_{rec}}{\text{TeV}}\right)$	Inner Galaxy region			Outer Galaxy region		
	$n=2.0$	$n=2.5$	$n=3.0$	$n=2.0$	$n=2.5$	$n=3.0$
1.0-1.2	11.37 ± 1.09	5.97 ± 0.67	3.56 ± 0.51	9.55 ± 3.03	4.58 ± 1.63	2.65 ± 1.22
1.2-1.4	8.77 ± 0.71	4.26 ± 0.43	2.42 ± 0.31	5.45 ± 1.00	2.25 ± 0.44	0.98 ± 0.20
1.4-1.6	8.14 ± 0.73	2.97 ± 0.36	1.37 ± 0.22	4.32 ± 0.66	1.39 ± 0.23	0.49 ± 0.09
1.6-1.8	6.66 ± 0.56	1.95 ± 0.21	0.76 ± 0.11	6.07 ± 1.30	1.88 ± 0.45	0.58 ± 0.15
1.8-2.0	6.56 ± 0.70	1.97 ± 0.27	0.87 ± 0.16	2.44 ± 0.45	0.77 ± 0.16	0.22 ± 0.05
>2.0	3.26 ± 0.23	0.76 ± 0.06	0.20 ± 0.02	1.47 ± 0.34	0.39 ± 0.09	0.10 ± 0.03

Diffuse emissions with significant detection

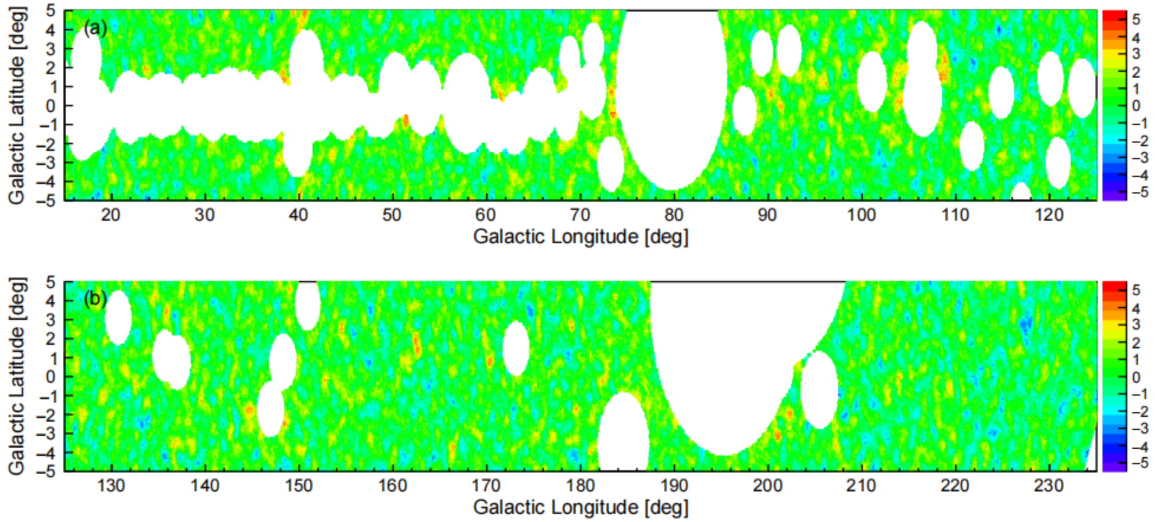

LHAASO Collaboration. (PRL, 2023)

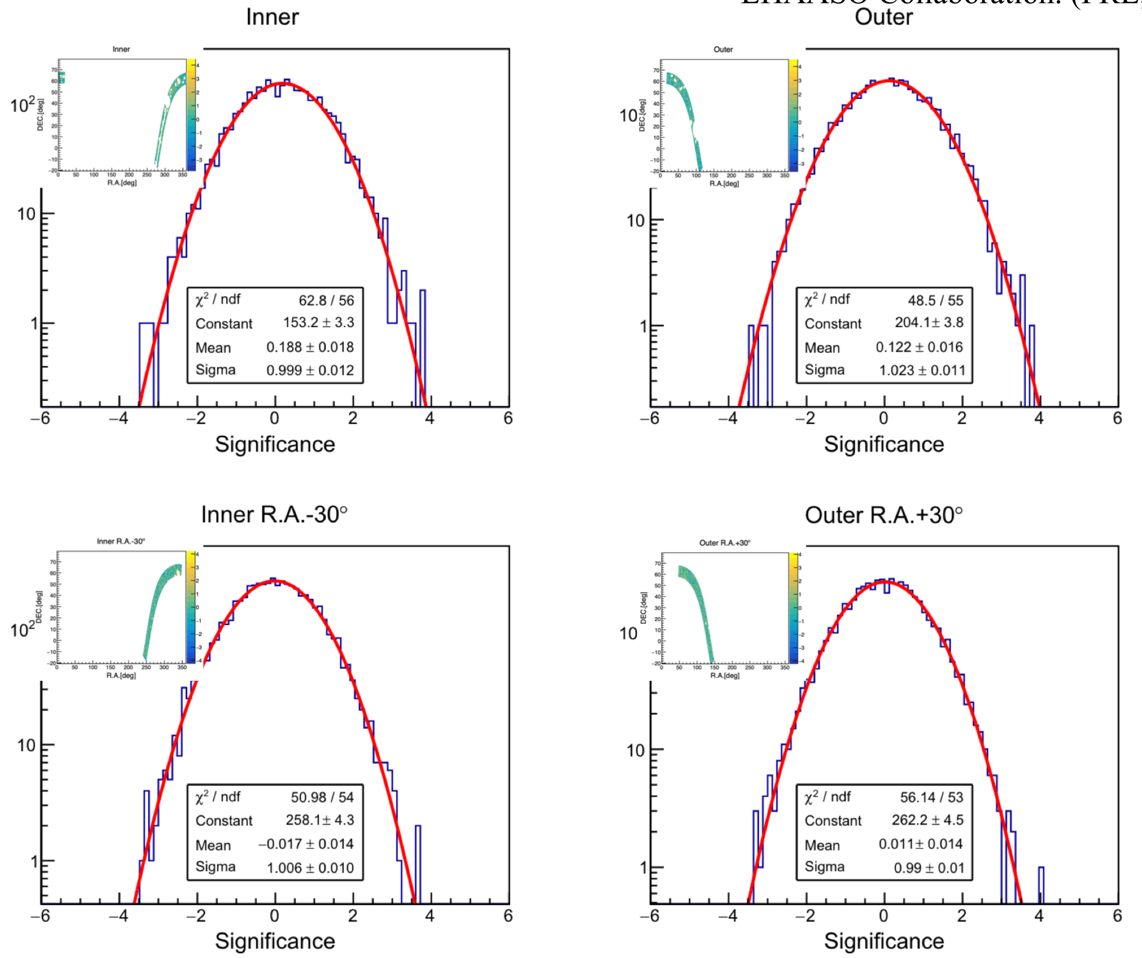

- No significant point source left on the significance map
- From 1-dimentional significance distributions, positive residuals in our ROIs, but standard Gaussian distributions for reference regions

LHAASO-KM2A diffuse results

LHAASO Collaboration. (PRL, 2023)

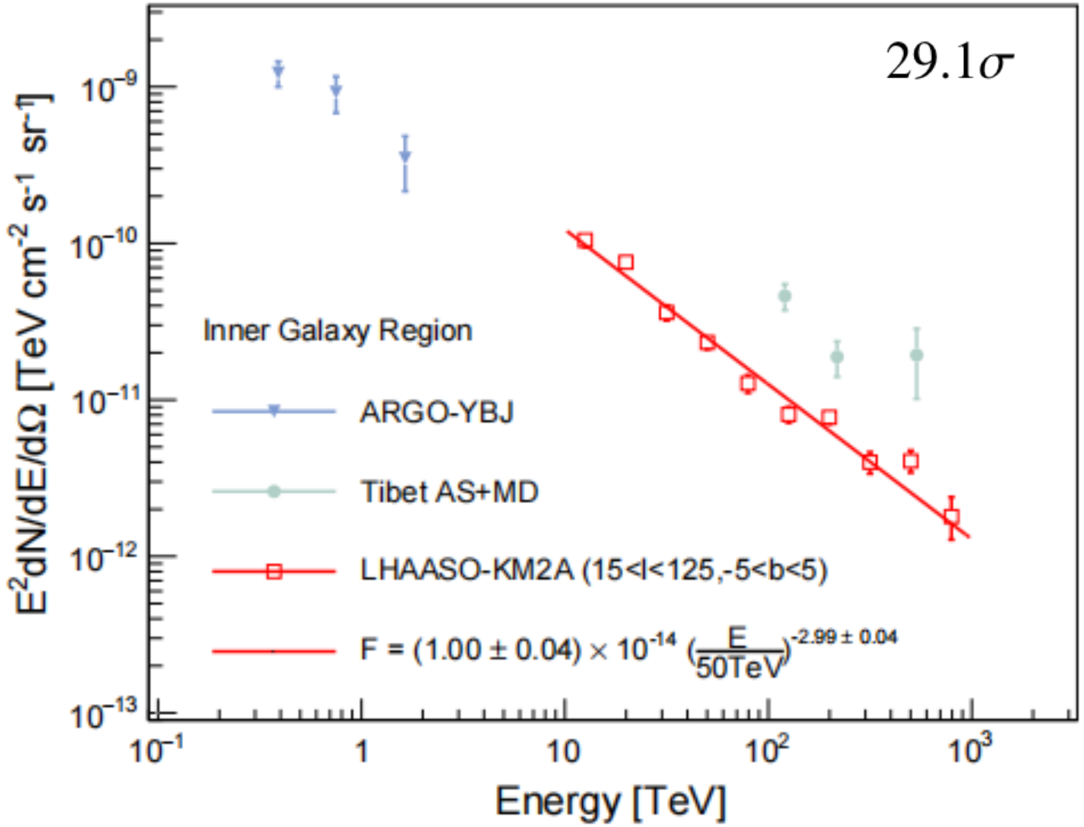

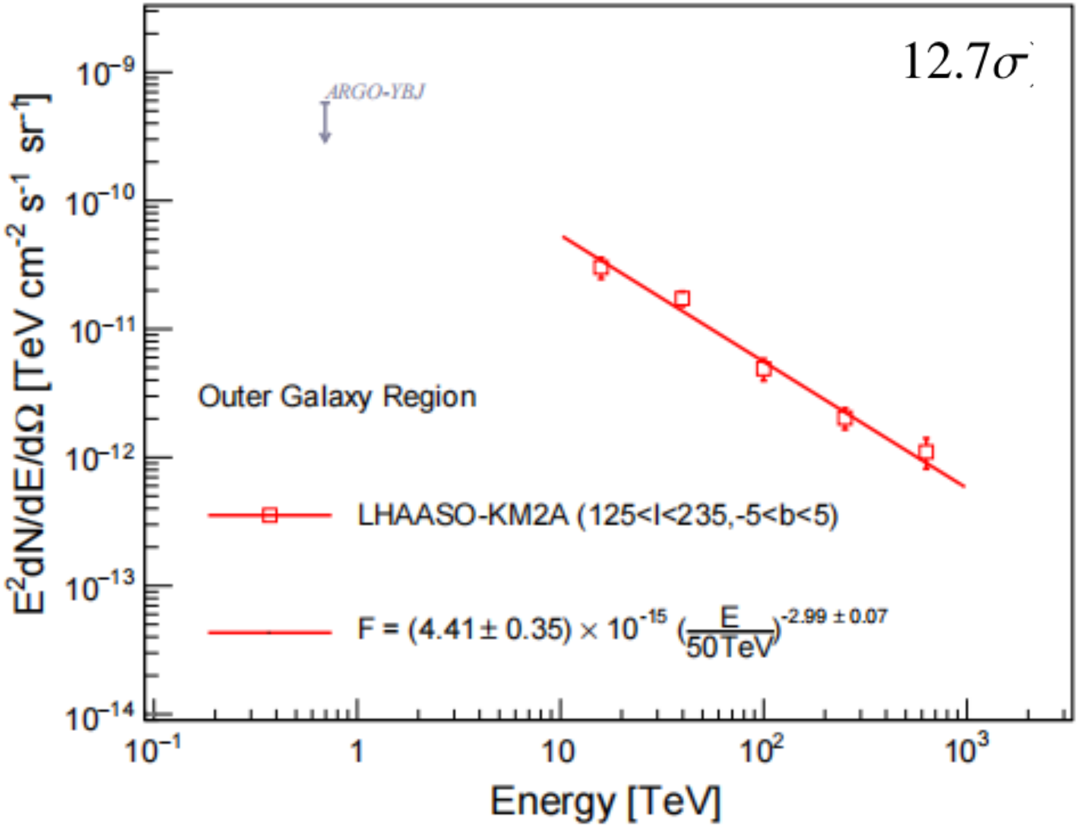

- First detection of VHE diffuse emission from outer Galactic plane
- Spectra follow power-law forms with an index of ~3

Longitude and latitude profiles

LHAASO Collaboration. (PRL, 2023)

10-63 TeV

63-1000 TeV

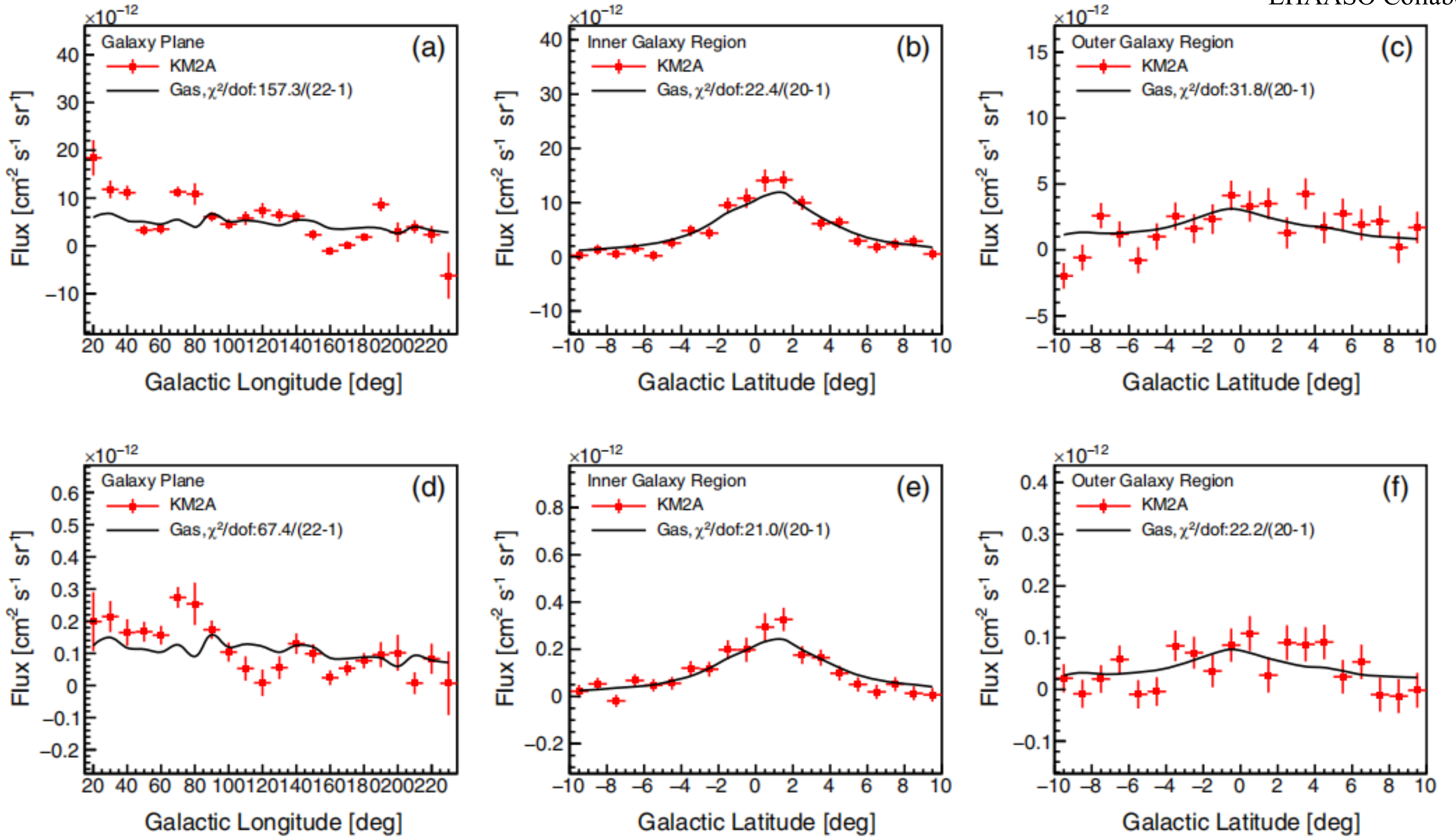

Roughly consistent with gas distributions for *b*, but show significant deviation for *l*

The gas distribution may not well trace the diffuse γ-ray emission at very high energies

Confront LHAASO-KM2A data with a toy model

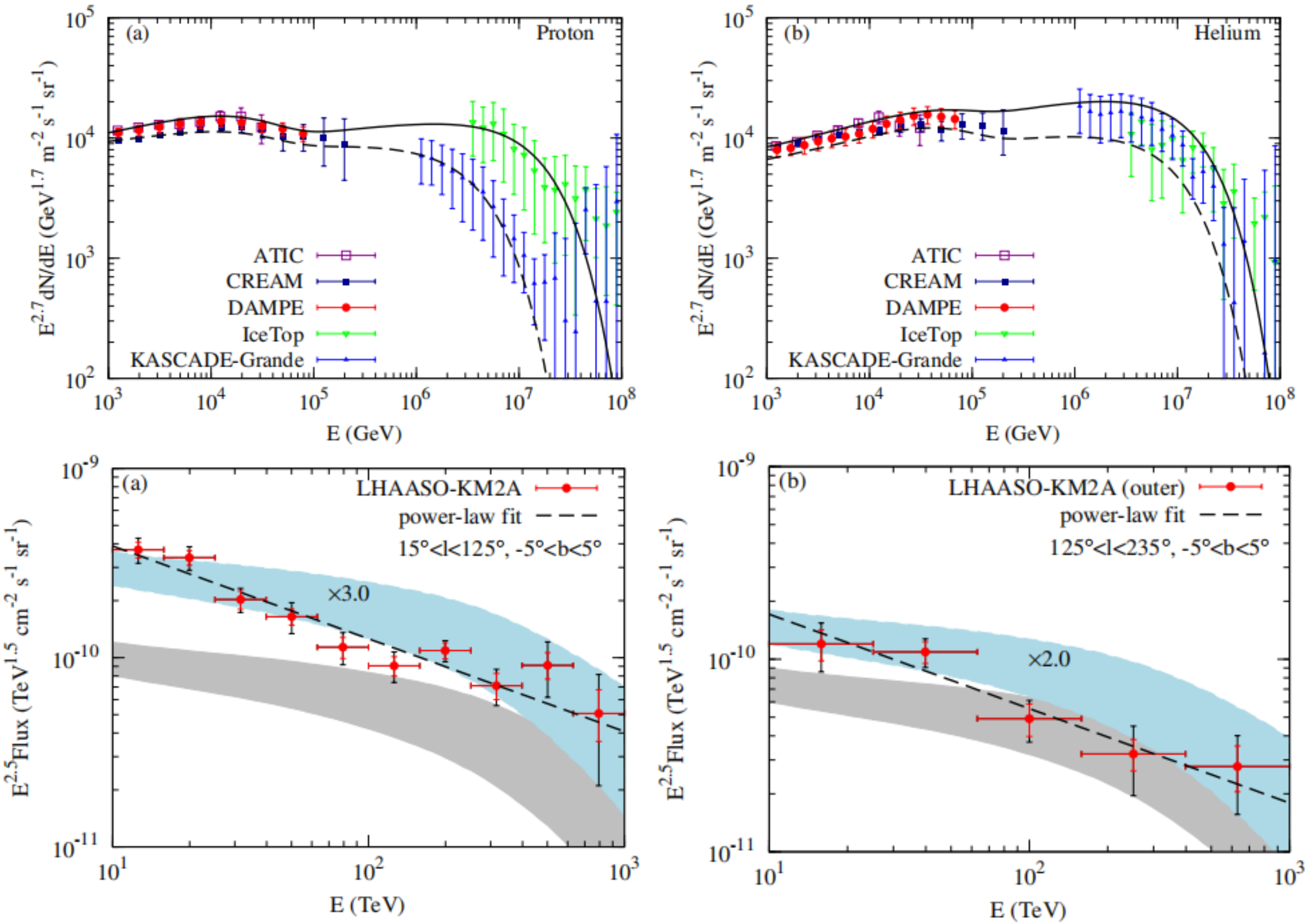

LHAASO Collaboration. (PRL, 2023)

- Toy model prediction: local CR × gas column (PLANCK dust opacity)
- Measured fluxes are higher by a factor of 2~3 than predictions: unresolved sources or propagation effect?

Diffuse emissions from Fermi-LAT observations

- Time cut: August 4, 2008 to March 2, 2023 (761 weeks)
- Energy cut: 1 GeV to 500 GeV
- ROIs: Inner Galaxy Region, Outer Galaxy Region
- Event class: P8R3 Ultracleanveto
- Other cuts: Zenith angle < 90 degree, (DATAQUAL>0)&&(LATCONFIG==1)

Data

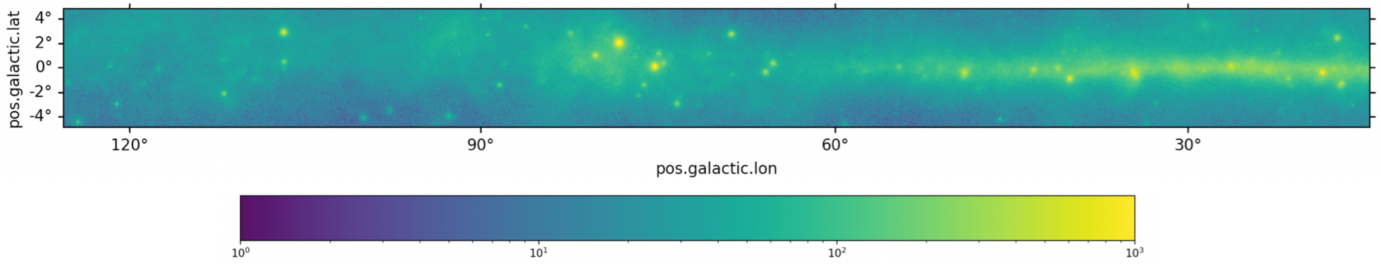

(Data-Psc-Iso)*Mask

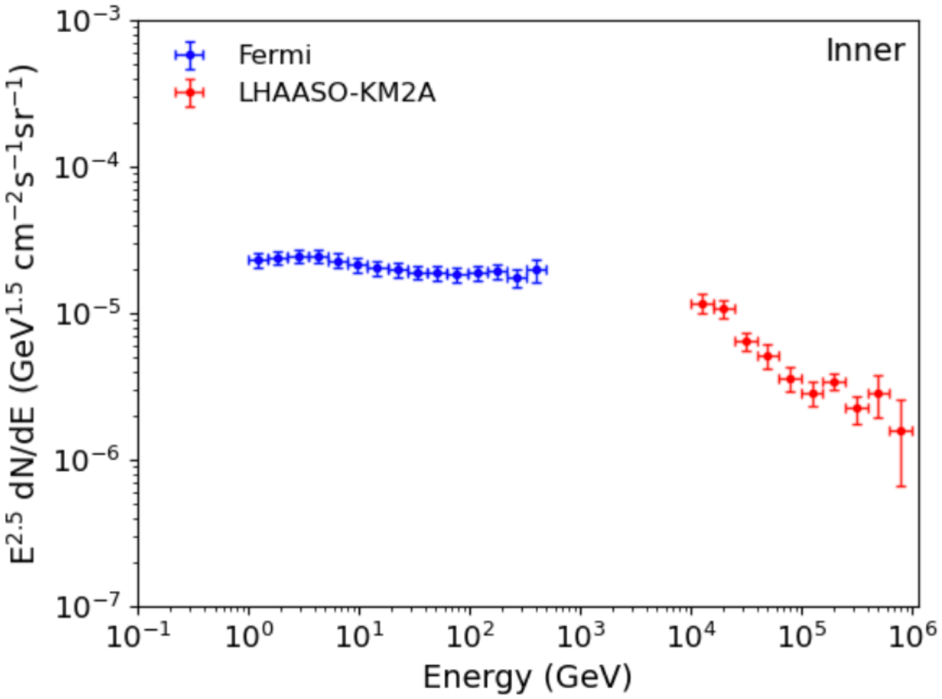

R. Zhang et al. (ApJ, 2023)

Confront wide-band observations with a GALPROP model

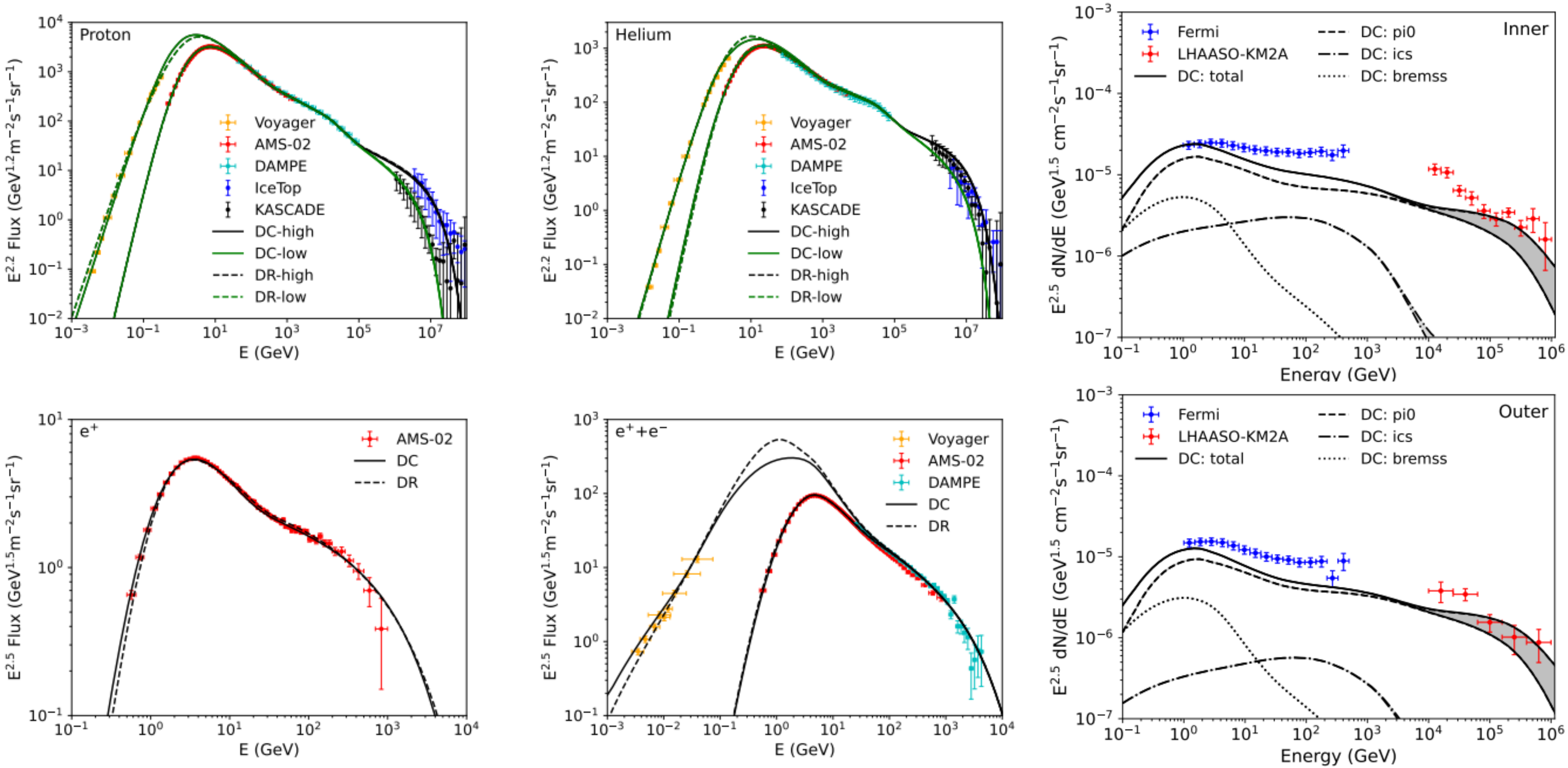

R. Zhang et al. (ApJ, 2023)

Unresolved source population?

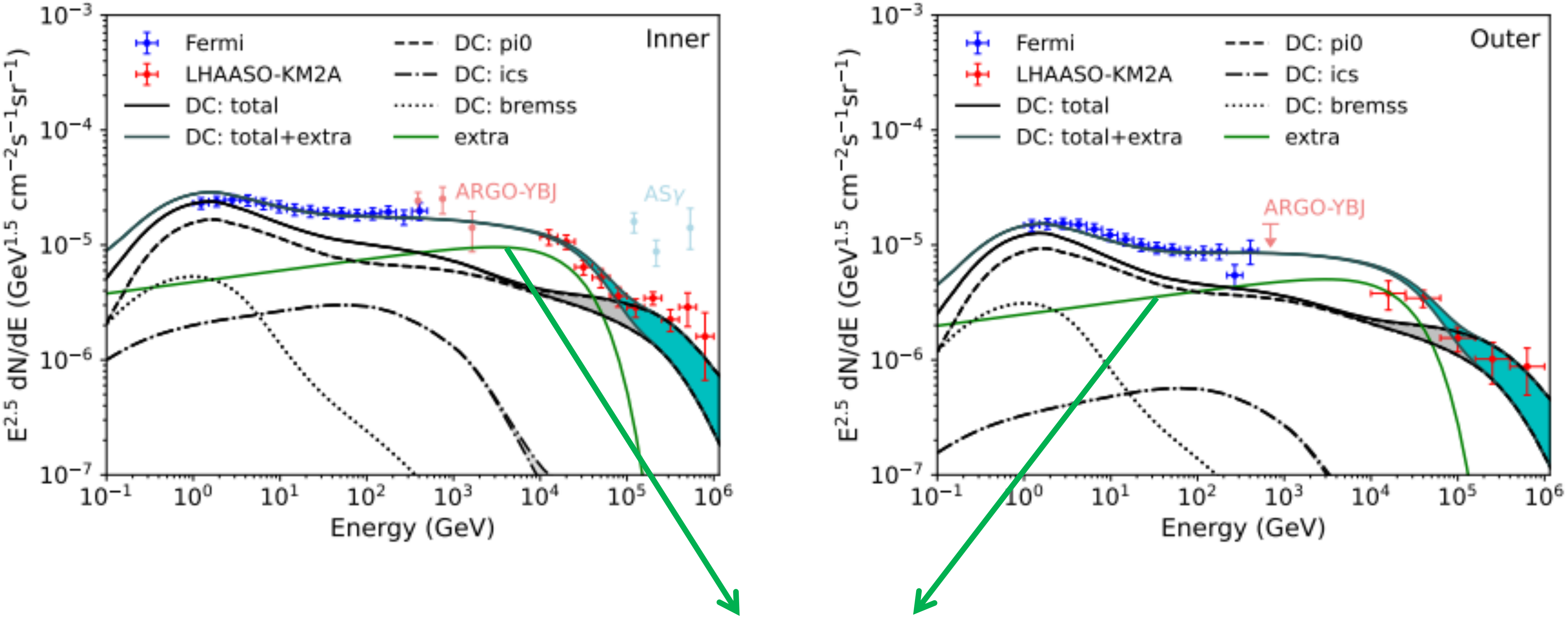

$$\propto E^{-2.40} \exp\left(-E/30\ \mathrm{TeV}\right)$$

$$f(r,z) = (r/r_\odot)^{1.25} \exp\left[-3.56(r-r_\odot)/r_\odot\right] \exp\left(-|z|/z_s\right)$$

R. Zhang et al. (ApJ, 2023)

More infromation from LHAASO-WCDA needed

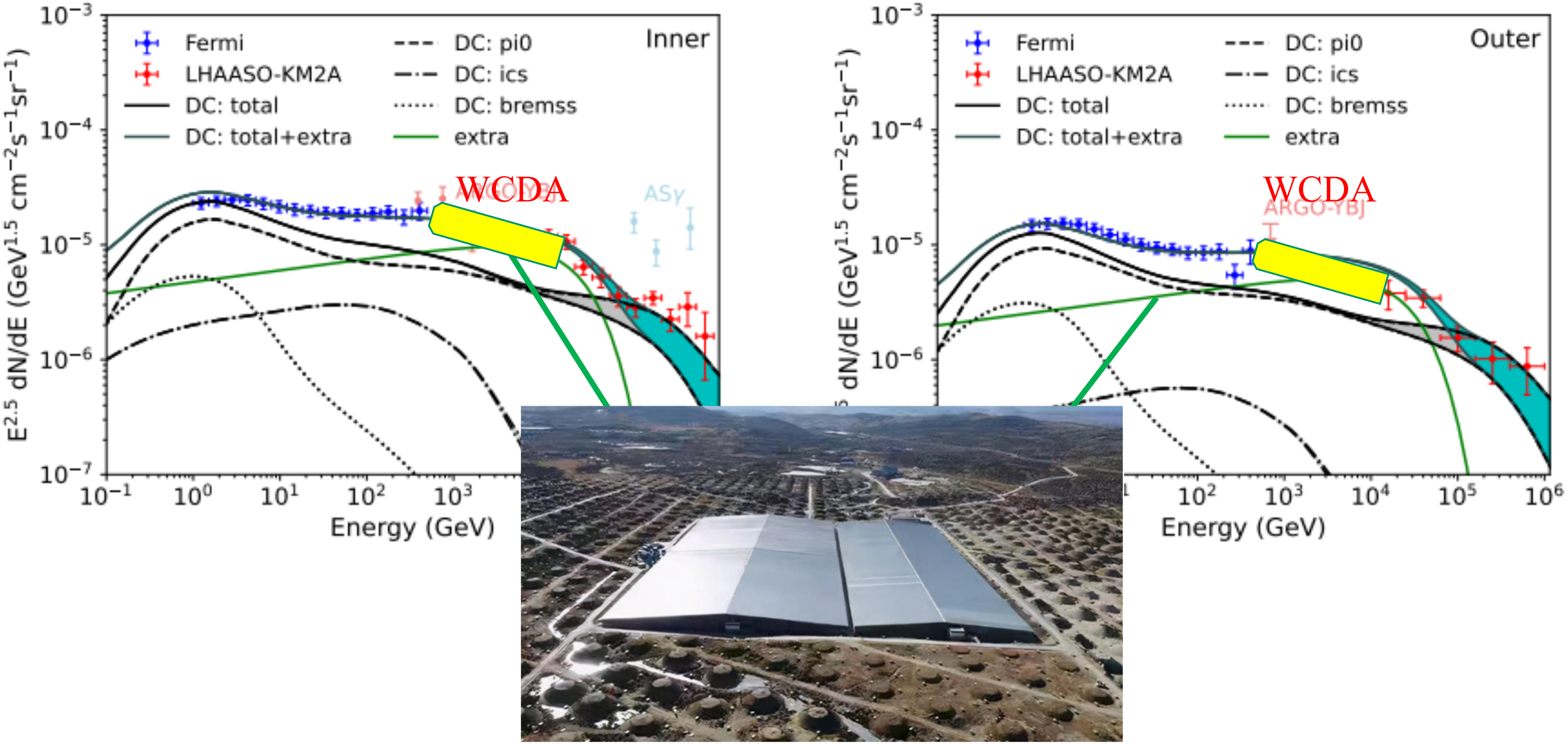

R. Zhang et al. (ApJ, 2023)

Summary

- The diffuse emission from two regions of the Galactic plane was observed with high significance; Firstly detected in the outer Galaxy region!
- Spectral indices of both regions are about -3; deviation from single power-law is not evident by the current data
- The latitude distributions are consistent with the gas template, and more complicated structures in the longitude distributions
- Overall fluxes of are higher by a factor of several than the local CR interaction with l.o.s. gas —— unresolved sources or propagation effect?
- Wide-band diffuse emissions show significant excesses, and a population of unresolved sources may have substantial contribution.

LHAASO Collaboration. (PRL, 2023)

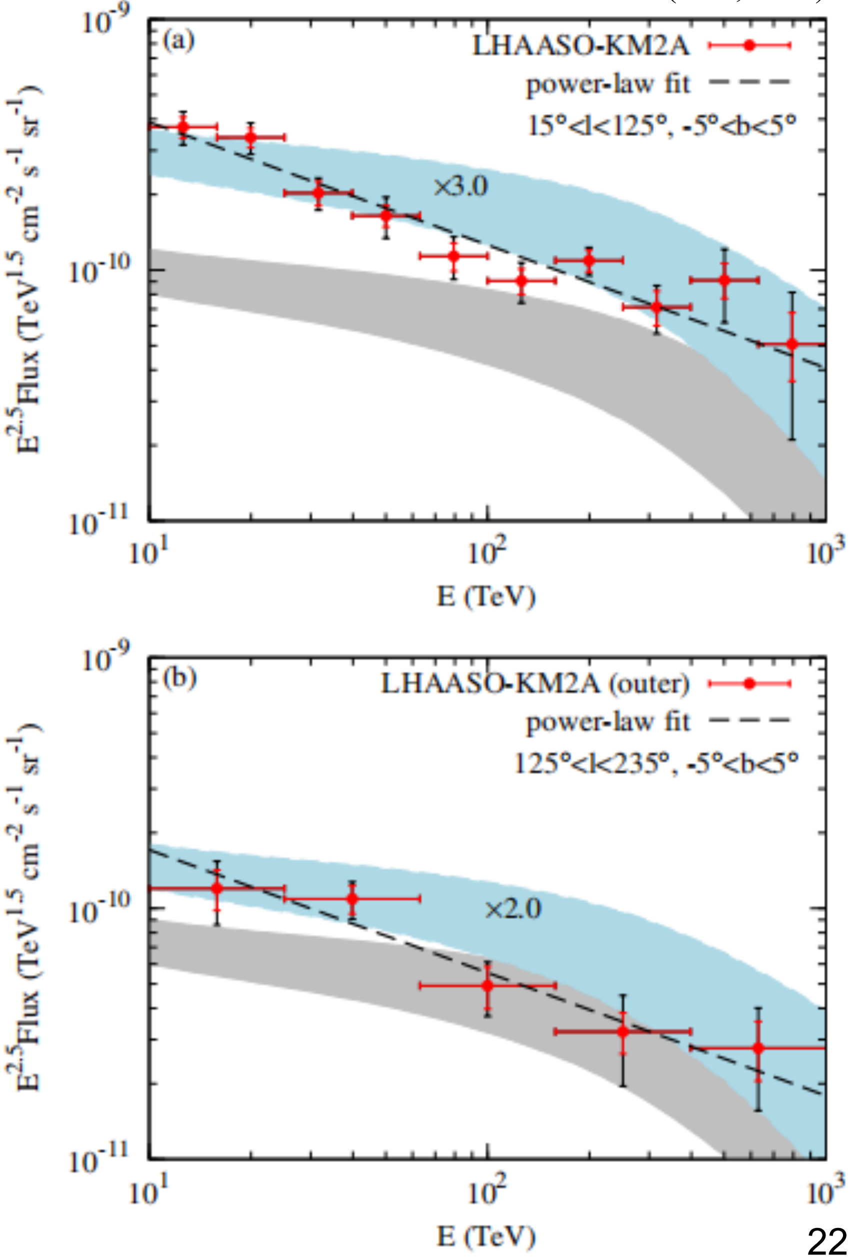

Thank you!

Residual source contamination

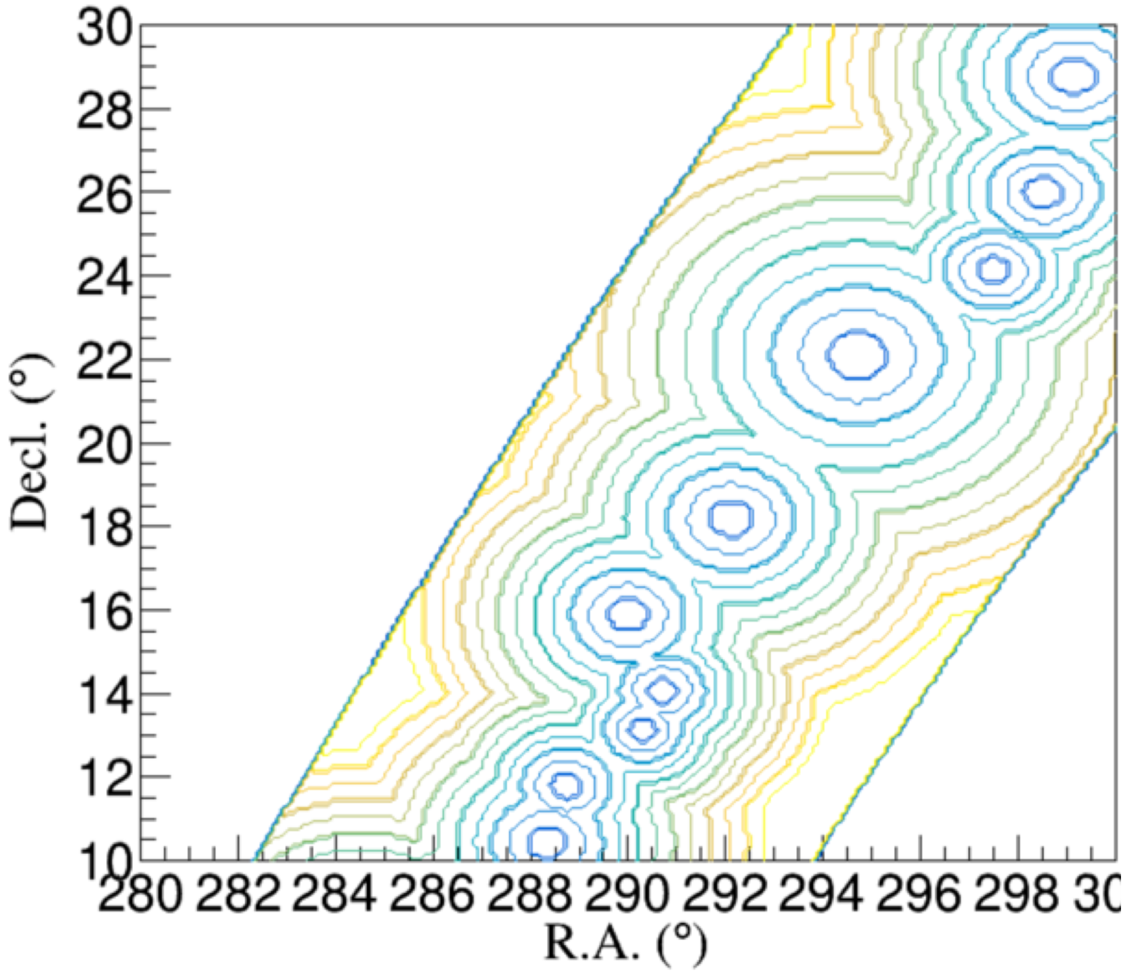

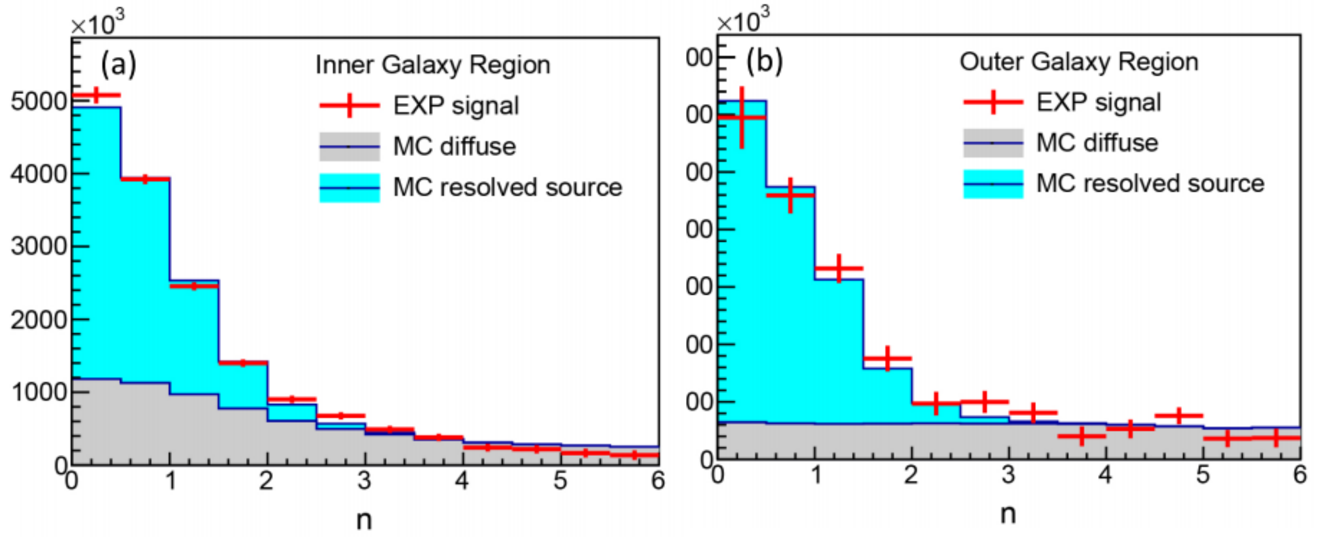

Table 5: Proportion (%) of contamination (f_{cont}) of residual sources (LHAASOCat+TeVCat) to the DGE.

$\log_{10}\left(\frac{E_{rec}}{\mathrm{TeV}}\right)$	Inner Galaxy region			Outer Galaxy region		
	$n = 2.0$	$n = 2.5$	$n = 3.0$	$n = 2.0$	$n = 2.5$	$n = 3.0$
1.0-1.2	11.37 ± 1.09	5.97 ± 0.67	3.56 ± 0.51	9.55 ± 3.03	4.58 ± 1.63	2.65 ± 1.22
1.2-1.4	8.77 ± 0.71	4.26 ± 0.43	2.42 ± 0.31	5.45 ± 1.00	2.25 ± 0.44	0.98 ± 0.20
1.4-1.6	8.14 ± 0.73	2.97 ± 0.36	1.37 ± 0.22	4.32 ± 0.66	1.39 ± 0.23	0.49 ± 0.09
1.6-1.8	6.66 ± 0.56	1.95 ± 0.21	0.76 ± 0.11	6.07 ± 1.30	1.88 ± 0.45	0.58 ± 0.15
1.8-2.0	6.56 ± 0.70	1.97 ± 0.27	0.87 ± 0.16	2.44 ± 0.45	0.77 ± 0.16	0.22 ± 0.05
>2.0	3.26 ± 0.23	0.76 ± 0.06	0.20 ± 0.02	1.47 ± 0.34	0.39 ± 0.09	0.10 ± 0.03

Systematic uncertainties

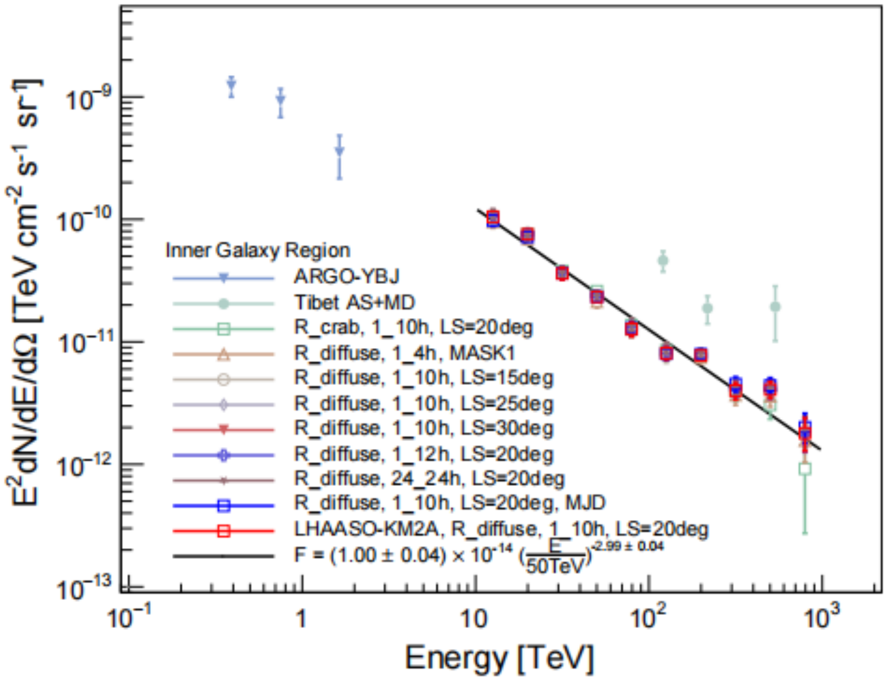

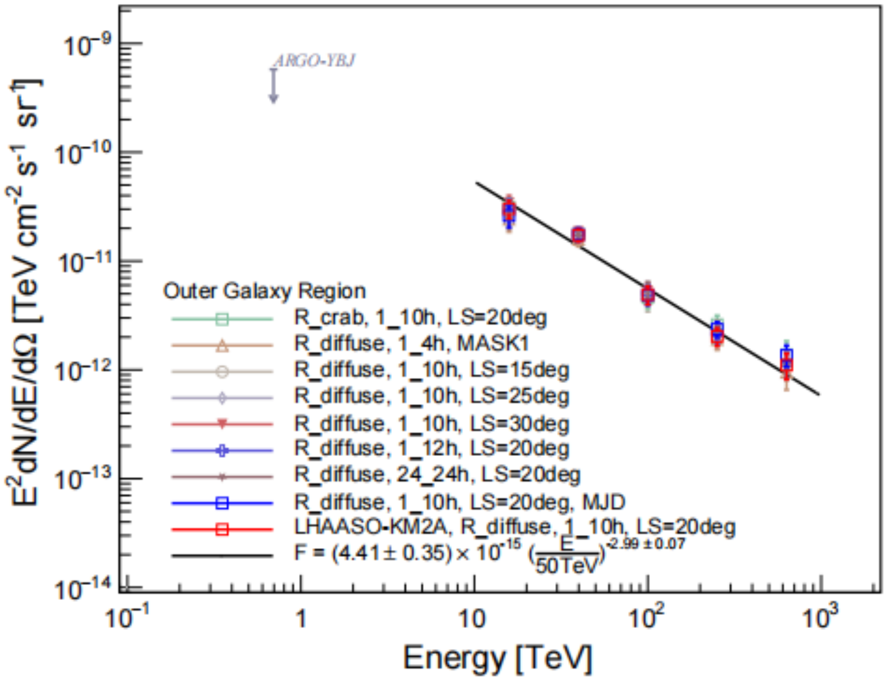

Spectrum results	Inner		Outer	
	Flux[a]	Index	Flux[a]	Index
Statistics	$1.00 \pm 0.04_{stat}$	$-2.99 \pm 0.04_{stat}$	$0.44 \pm 0.04_{stat}$	$-2.99 \pm 0.07_{stat}$
Layout	1%	0.02	1%	0.02
γ/CR Discrimination	2%	0.04	5%	0.06
Background Estimation	5%	0.05	10%	0.10
Atmospheric Model	7%	0.02	7%	0.02
Overall	9%	0.07	12%	0.12

Test with Tibet-ASγ's mask

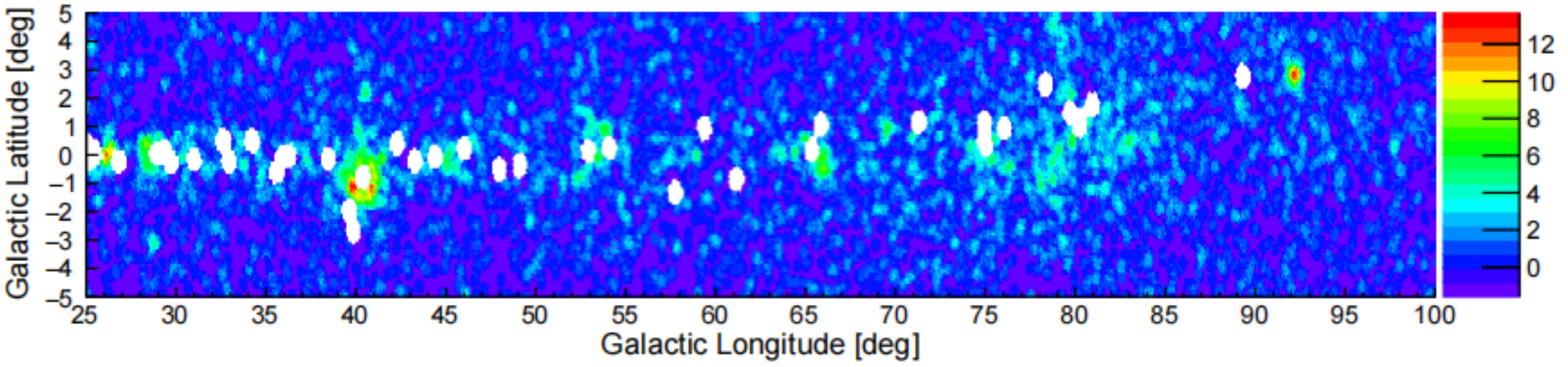

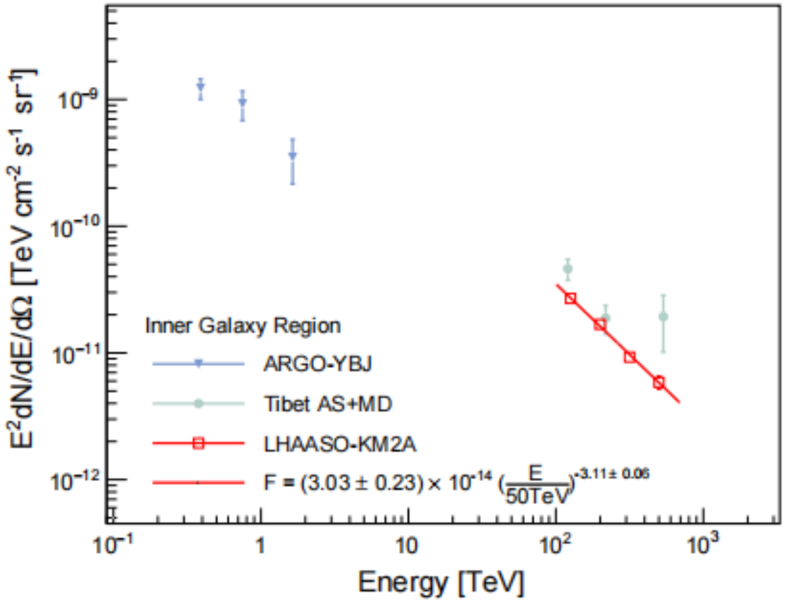

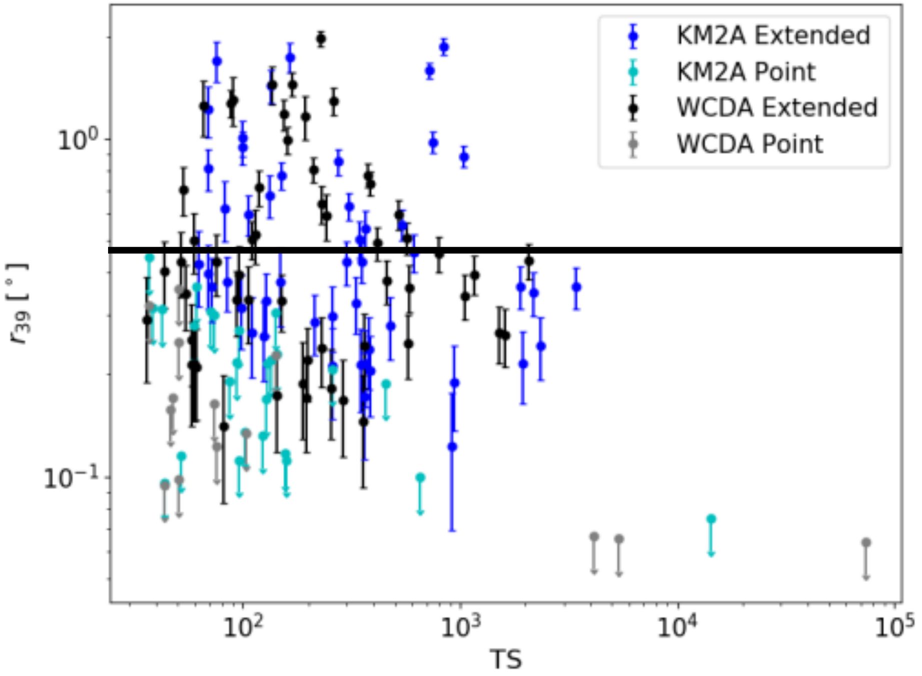

VHE diffuse emission by HAWC

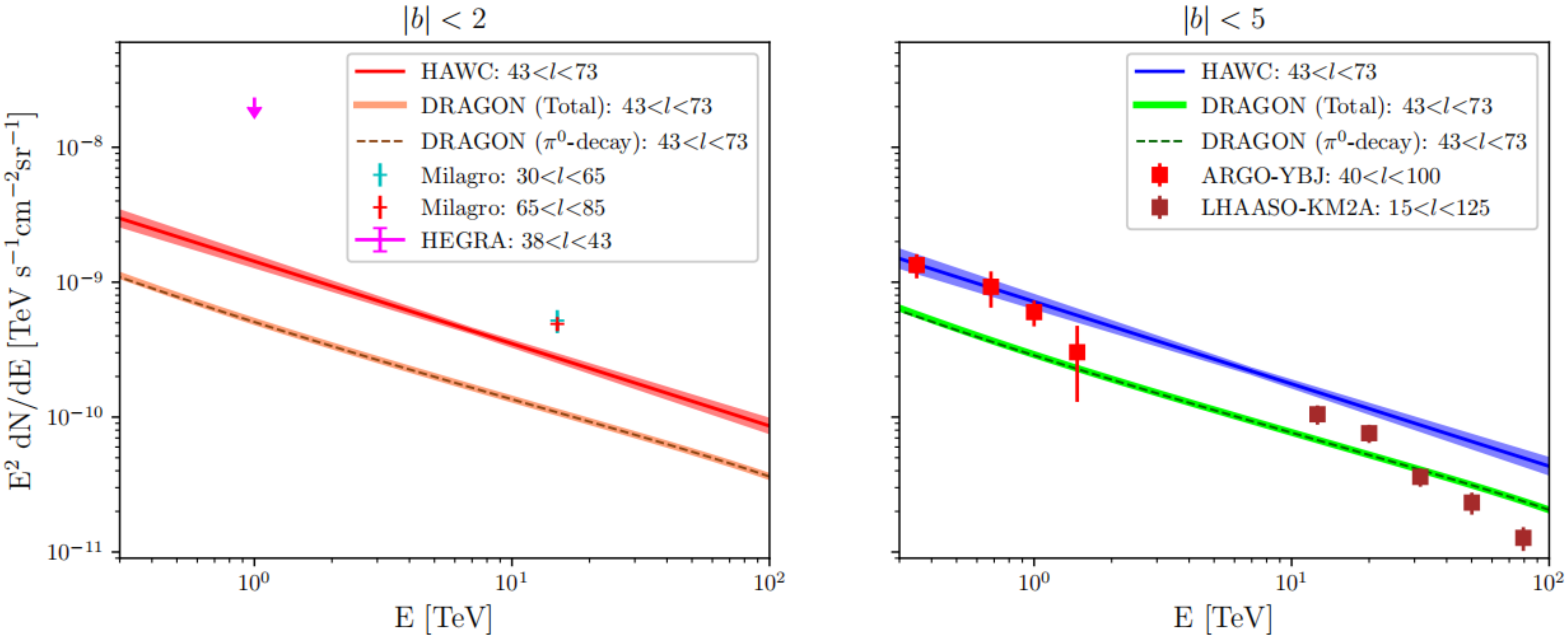

spectrum is compatible with the spectrum of the emission arising from a CR population with an *index* similar to that of the observed CRs. When comparing with the DRAGON *base model*, the HAWC GDE flux is higher by about a factor of 2. Unresolved sources such as pulsar wind nebulae and teraelectronvolt halos could explain the excess

HAWC 2024, ApJ, 961, 104